Study of Symmetries from $N_f = 2$ and $N_f = 2 + 1$ in finite temperature QCD using Möbius Domain Wall Fermions

David Ward[1]

[1]Department of Physics
National Taiwan University

Lattice Field Theory at the Frontier of Nuclear and Particle Physics
November 3rd, 2026



Symmetry of screening masses of mesons in two-flavor lattice QCD at high temperatures

Y. Aoki,[1] H. Fukaya,[2] S. Hashimoto,[3,4] I. Kanamori,[1] Y. Nakamura,[1] C. Rohrhofer,[2] K. Suzuki,[5] and D. Ward[2]

(JLQCD Collaboration)

[1]*RIKEN Center for Computational Science, 7-1-26 Minatojima-minami-machi, Chuo-ku, Kobe, Hyogo 650-0047, Japan*
[2]*Department of Physics, The University of Osaka, Toyonaka 560-0043, Japan*
[3]*High Energy Accelerator Research Organization (KEK), Tsukuba 305-0801, Japan*
[4]*School of High Energy Accelerator Science, The Graduate University for Advanced Studies (Sokendai), Tsukuba 305-0801, Japan*
[5]*Advanced Science Research Center, Japan Atomic Energy Agency (JAEA), Tokai 319-1195, Japan*

(Received 29 January 2025; accepted 16 May 2025; published 13 June 2025)

We investigate spatial two-point correlation functions of mesonic operators in two-flavor lattice QCD at high temperatures. The simulated temperatures cover the range $T \in [147, 330]$ MeV, where the critical temperature is estimated around 165 MeV. To ensure a good control of the chiral symmetry we employ the Möbius domain-wall fermion action for two degenerate flavors of quarks. With a lattice cutoff $a^{-1} \sim 2.6$ GeV, the residual mass is reduced to 0.14 MeV. With the energy spectrum obtained from the screening mass at incremental values of the temperature range, we examine the $SU(2)_L \times SU(2)_R$ chiral symmetry, the anomalous axial $U(1)$, as well as an enhanced symmetry which exchanges the spin degrees of freedom. We also study how the data approaches the perturbative prediction given by twice the Matsubara frequency of free quarks.

DOI: 10.1103/yh8j-q93c

Table of Contents

1. Introduction
2. Quantum Chromodynamics and Chiral Symmetry
3. Lattice field theory and Möbius Domain Wall fermions
4. Symmetries of QCD from the Screening Mass of the 2-pt Correlation Function
5. Numerical Analysis
6. Conclusion

Introduction

Some Motivation to Study Chiral Symmetry

- Chiral symmetry, which broke spontaneously in the early universe, is a critical input in the $\mathcal{O}(1)$GeV mass of hadrons.
- Restoration of chiral symmetry at high temperatures is predicted to occur.
- High temperature quark phenomena such as deconfinement are linked to chiral symmetry.
- Despite the chiral phase transition occurring in the early universe, details of the high temperature symmetries are not well known.

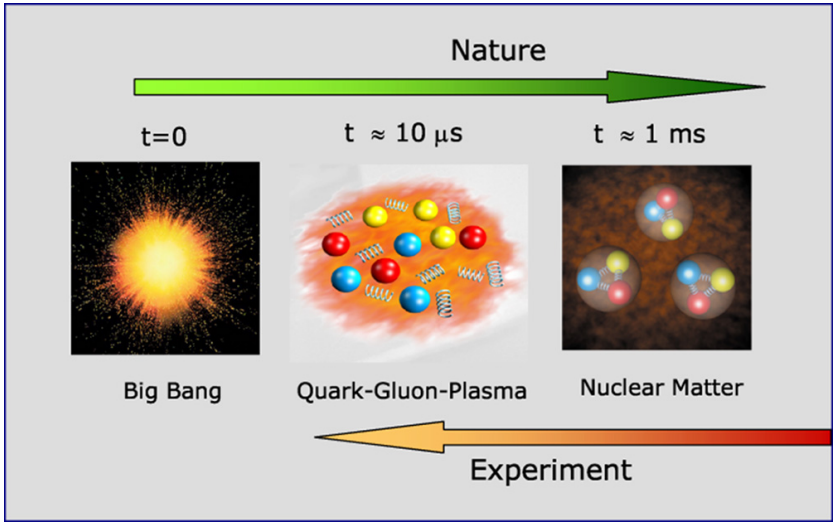

From NTNU webpage

Goals

- For finite temperature QCD in the range of $T = 138 - 330\text{MeV}$, we have three target symmetries of interest:

Symmetries of Lagrangian	
$SU(2)_L \times SU(2)_R$	Standard chiral symmetry; *origin of hadron mass*
$U(1)_A$	Broken explicitly by quantum anomaly, anomaly breaking may be suppressed at $T > T_c$
Emergent Symmetry due to Heavy Matsubara Mass	
$SU(2)_{CS}$	*May* emerge at very high temperatures (predicted by Laine et al. [1])

- Möbius Domain Wall fermions offer a clean theoretical analysis of these symmetries due to good chiral symmetry with a precision of five digits.

[1] Laine and Vepsalainen . *JHEP*. **02**. P. 004. 2004 [arXiv:hep-ph/0311268]

Comparisons with other collaborations

- Symmetries around the chiral crossover have been the target of numerous studies.
- A selection of studies with temperatures around the chiral crossover are listed below.

Collaboration	B.Brandt et al. [2]	HotQCD [3]	T.W.Chiu [4, 5, 6]	
N_f	2	2+1	2+1+1	
Year	2016	2019	2023,24	2026
Fermion Operator	Wilson	Staggered	Möbius Domain Wall	
Symmetry	$SU(2)_V \times U(1)_V$	$U(1)_{V'} \times U(1)_{A'} \times U(1)_V$	$SU(2)_L \times SU(2)_R \times U(1)_V$	
a[fm]	0.08	0.017-0.234	0.0641,0.0685	0.064-0.075
Estimated Chiral Symmetry Breaking	$aT_c \leq 0.067$	$aT_c \leq 0.18$	$am_{res} \leq 1.9 \times 10^{-5}$	$am_{res} = 1.0 \times 10^{-6} - 6.2 \times 10^{-5}$

JLQCD Study	Fixed β	Line of Constant Physics
N_f	2	2+1
Year	2025	
Fermion Operator	Möbius Domain Wall	
Symmetry	$SU(2)_L \times SU(2)_R \times U(1)_V$	
a[fm]	0.075	$N_t = 12$: 0.0804-0.126 $N_t = 16$: 0.0493-0.089
Estimated Chiral Symmetry Breaking	$am_{res} = 5.3 \times 10^{-5}$	$N_t = 12$: $m_{res} = 4.15 \times 10^{-4} - 5.913 \times 10^{-3}$ $N_t = 16$: $m_{res} = 8 \times 10^{-6} - 8.14 \times 10^{-4}$

[2] Brandt et al. *JHEP*. **12**. P. 158. 2016 [arXiv:1608.06882]
[3] Bazavov et al. *Phys. Rev. D*. **100**. P. 094510. 2019 [arXiv:1908.09552]
[4, 5, 6] Chiu . *Phys. Rev. D*. **107**. P. 114501. 2023 [arXiv:2302.06073], Chiu . *Phys. Rev. D*. **110**. P. 014502. 2024 [arXiv:2404.15932], Chiu and Hsieh [arXiv:2602.14811]

Overview

- JLQCD simulated $N_f = 2$, and $N_f = 2 + 1$ QCD using Möbius domain-wall fermions with $m_{res} < 1\text{MeV}$ for both fixed beta and along a line of constant physics.
- Using Möbius domain-wall fermions is theoretically clean with well defined $SU(2)_L \times SU(2)_R$ and axial $U(1)_A$ symmetries.
- Prior work by JLQCD [7] focused on temperatures above $1.1\,T_c$, and used a proportion of spatial correlators to study symmetries of QCD.
- This talk focuses on the fixed beta $N_f = 2$ and $N_f = 2 + 1$ line of constant physics studies which are centered around T_c and use screening mass differences of the mesonic spatial correlators.

[7] Rohrhofer et al. *Phys. Rev. D.* **100**. P. 014502. 2019 [arXiv:1902.03191]

Quantum Chromodynamics and Chiral Symmetry

Chiral Symmetry in the Lagrangian

- In addition to gauge symmetry, the QCD Lagrangian can be shown to have chiral symmetry in the limit $m \to 0$,

$$\mathcal{L} = \bar{\psi}(x) i \not{D} \psi(x) - m \bar{\psi}(x) \psi(x).$$

- Applying the chiral projectors

$$P_L = \frac{1 - \gamma_5}{2}, \quad P_R = \frac{1 + \gamma_5}{2}.$$

$$\psi_R(x) = P_R \psi(x) \qquad \bar{\psi}_R(x) = \bar{\psi}(x) P_L,$$
$$\psi_L(x) = P_L \psi(x) \qquad \bar{\psi}_L(x) = \bar{\psi}(x) P_R.$$

- The chiral symmetry of the Lagrangian is more clear,

$$\mathcal{L} = i \bar{\psi}_R \not{D} \psi_R + i \bar{\psi}_L \not{D} \psi_L - m(\bar{\psi}_R \psi_L + \bar{\psi}_L \psi_R).$$

- The primary structure of $SU(N_f)_L \times SU(N_f)_R$ is determined by the u, d quarks as these are approximately chiral and degenerate.

$$\begin{aligned}
\psi &\to e^{i\theta_{aL}\tau^a_L/2}\psi, & \bar{\psi} &\to \bar{\psi}e^{-i\theta_{aL}\tau^a_L/2}, & SU(2)_L,\\
\psi &\to e^{i\theta_{aR}\tau^a_R/2}\psi, & \bar{\psi} &\to \bar{\psi}e^{-i\theta_{aR}\tau^a_R/2}, & SU(2)_R,\\
\psi &\to e^{i\gamma_5\theta}\psi, & \bar{\psi} &\to \bar{\psi}e^{i\gamma_5\theta}, & U(1)_A,\\
\psi &\to e^{i\theta}\psi, & \bar{\psi} &\to \bar{\psi}e^{-i\theta}, & U(1)_V
\end{aligned}$$

  where $F \in \{F^s, F^n\}, \quad F^s = \mathbb{I}, \quad F^n \in \{\tau^a/2\}$.
- This means that the spinors ψ and $\bar{\psi}$ transform under a total chiral symmetry

$$SU(2)_L \times SU(2)_R \times U(1)_A \times U(1)_V,$$

  for $N_f = 2$ and $N_f = 2 + 1$.
- These symmetries are exact symmetries of the Lagrangian in the chiral limit ($m \to 0$).

- The chiral condensate $\langle \bar{\psi}\psi \rangle$ is the order parameter for spontaneous breaking of $SU(2)_L \times SU(2)_R$.

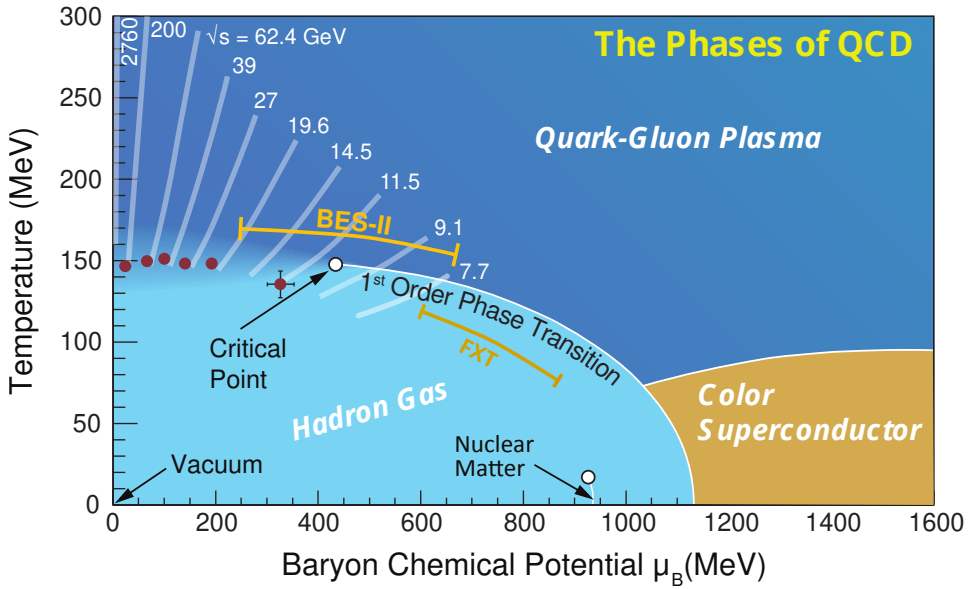

M. Stephanov – [8]

- $\langle \bar{\psi}\psi \rangle \neq 0$ contributes to the mass of low temperature hadrons and mesons through the Gell-Mann-Oakes-Renner relation

$$m_\pi^2 = -2\frac{m_u + m_d}{F_\pi^2} \langle \bar{\psi}\psi \rangle \,, \qquad \text{we expect } m_\pi(T) > m_\pi(0).$$

[8] Stephanov . *EPJ Web Conf.* **314**. P. 00042. 2024 [arXiv:2410.02861]

- $U(1)_A$ is broken explicitly by quantum anomaly at all energy scales.

$$Q_T = n_L - n_R, \quad \chi_T = \frac{Q_T^2}{V}, \quad \chi_T = \frac{\langle \bar{\psi}\psi \rangle}{mV} - \chi_{PS^0}$$

- Topological charge fluctuation is connected to gluon excitation and may be suppressed at high temperatures for physical *ud* quarks.

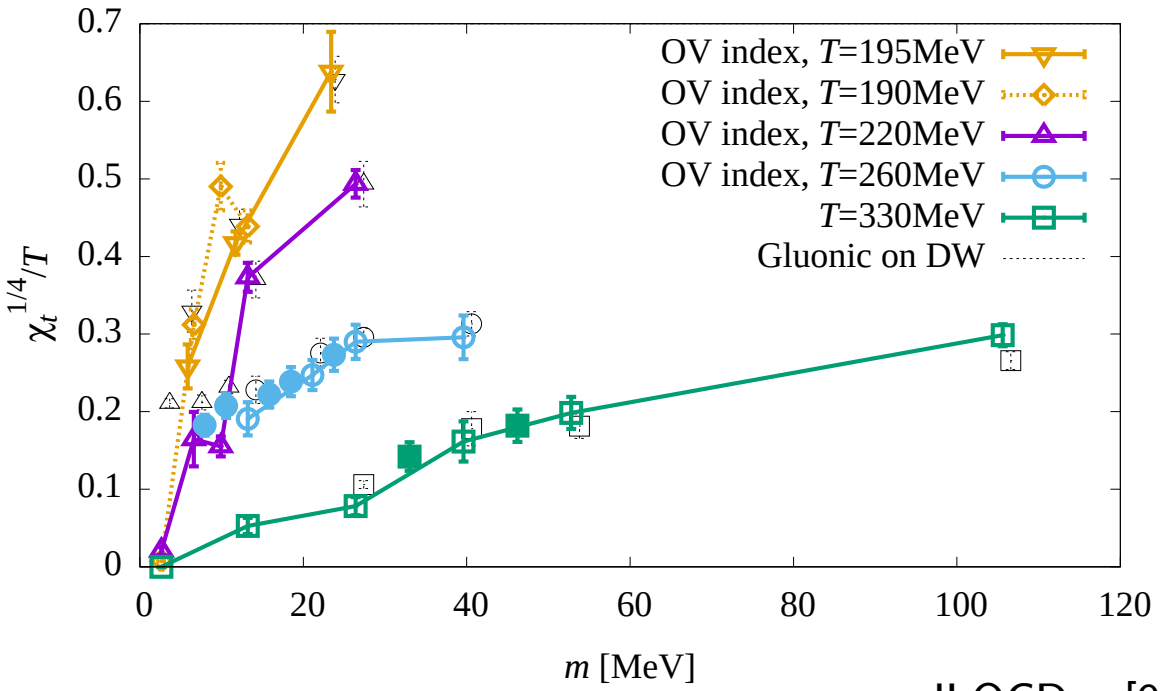

JLQCD – [9]

[9] Aoki et al. *Phys. Rev. D.* **103**. P. 074506. 2021 [arXiv:2011.01499]

Emergence of $SU(2)_{CS}$ for heavy Matsubara frequency

For $T \to \infty$ we expect the emergence of an additional symmetry, consider the free quark propagator along z:

$$\langle \bar{q}(z) q(0) \rangle (p_1, p_2) = \sum_{p_0} \int_{-\infty}^{\infty} \frac{dp_z}{(2\pi)} \frac{m - (i\gamma_0 p_0 + i\gamma_i p_i)}{p_0^2 + \delta_{ij} p_i p_j + m^2} e^{ip_3 z}$$

For $p_0 = (2n+1)\pi T$, the associated Matsubara frequency coming from the antiperiodic condition; when $T \gg m, p_1, p_2$ the propagator takes the form:

$$\langle \bar{q}(z) q(0) \rangle = \gamma_3 \frac{1 + i\mathrm{sgn}(p_0)\gamma_0\gamma_3}{2} e^{-\pi T z} + \mathcal{O}(1/T)$$

This quark propagator is invariant under the set of transformations:

$$\begin{aligned} q(x) &\to e^{i\Sigma^a \theta^a} q(x), \\ \bar{q}(x) &\to \bar{q}(x) \gamma_0 e^{i\Sigma^a \theta^a} \gamma_0, \end{aligned} \qquad \Sigma = \begin{bmatrix} \gamma_5 \\ \gamma_1 \\ i\gamma_1\gamma_5 \end{bmatrix}$$

forms the so-called chiral spin $SU(2)_{CS}$ group.

Lattice field theory and Möbius Domain Wall fermions

Overlap Operator and Domain Wall Fermions

- The Wilson operator removes doublers but explicitly breaks chiral symmetry.

$$S_W = -\frac{1}{2}\sum_{x,\mu} \bar{\psi}(x)(r-\gamma_\mu)U_\mu(x)\psi(x+\hat{\mu}) + \bar{\psi}(x+\hat{\mu})(r+\gamma_\mu)U_\mu^\dagger(x)\psi(x) + (\hat{M}_0+4r)\sum_x \bar{\psi}(x)\psi(x)$$

- If we consider operators which respect the Ginsparg-Wilson relation

$$\{D,\gamma_5\} = aDR\gamma_5 D,$$

we get a double free operator and we recover

$$\{D,\gamma_5\} = 0,$$

in the continuum and preserve a type of chiral symmetry on the lattice

$$\{D,\gamma_5(1-\frac{1}{2}aD)\} = 0.$$

- The matrix form of the Wilson operator can be used to construct an operator which satisfies the GW relation, the overlap operator

$$D_{OV} = m\left(1 + \frac{D_W(-M)}{\sqrt{D^\dagger D}}\right).$$

  When $m \to 0$ the overlap operator describes a chiral symmetry in the continuum limit.
- The Overlap operator preserves an exact chiral symmetry, but is derived as a kind of infinite limit from the 5D domain wall operator.
- We can, therefore, produce an excellent approximation to this operator using domain wall fermions for a sufficently long 5D extension.

This 5D operator, is called the Domain Wall fermion operator,

$$S_{DW} = \sum_x \sum_{s,s'} \bar{\psi}(x,s)[D_W^5(s,s') - \delta_{s,s'}M + m(P_L\delta_{s,L_s;1,s'} + P_R\delta_{s,1;L_s,s'})]\psi(x,s')$$

where M is treated as the height of the domain wall, m is the particle mass and the fermions are subject to the boundary condition:

$$\psi(x,0) = 0, \quad \psi(x,L_s+1) = 0.$$

This fifth dimension is not periodic and our physical chiral fermions correspond to the edges of the 5D bulk.

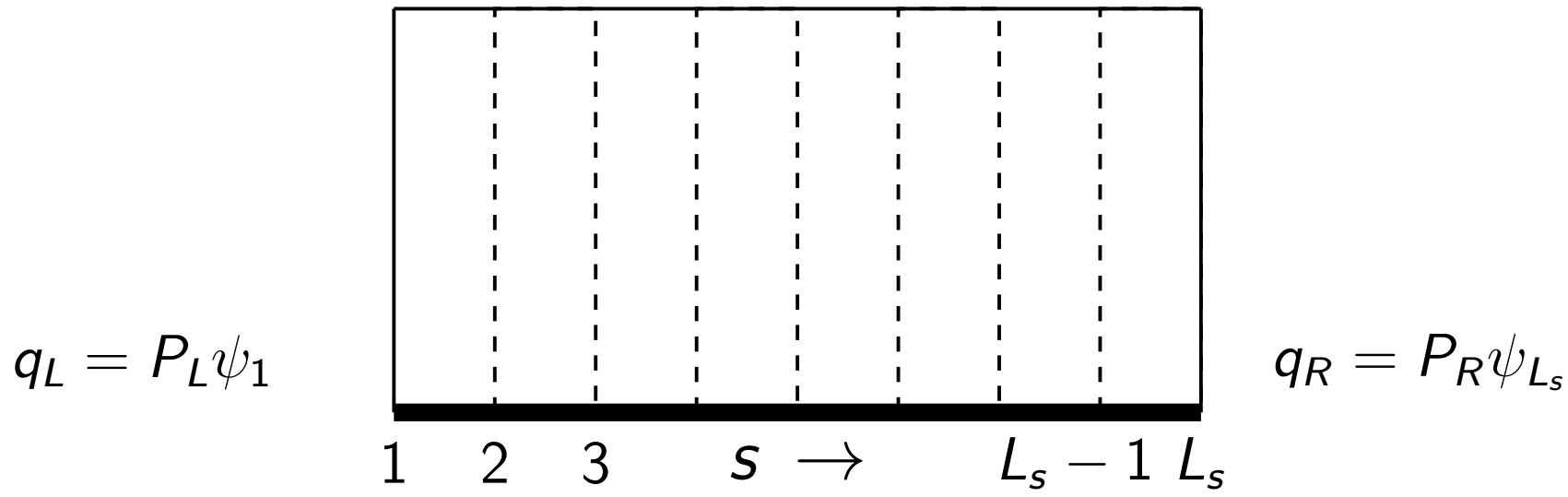

Brower – [10]

[10] Brower et al. *PoS.* **LATTICE2008**. P. 034. 2008 [arXiv:0906.2813]

- $\det[D^{5d}] \propto \det[D^{4d}]$ and can be written exactly following Pauli-Villars regularization.
- The form of the 4D operator corresponds to the form of Neuberger's overlap operator

$$D_{4D} = \frac{1+m}{2} + \frac{1-m}{2}\gamma_5 \epsilon(H_M).$$

- Where the sign function is approximated to be tanh-like

$$\epsilon(H_M) = \frac{(H_M+1)^{L_s} - (H_M-1)^{L_s}}{(H_M+1)^{L_s} + (H_M-1)^{L_s}} = \tanh[L_s \tanh^{-1}(H_M)].$$

  L_s is the extent of the fifth dimension.
- As $L_S \to \infty$, $\epsilon(H_M) \to \mathrm{sgn}(H_M)$ and we get an exact symmetry

$$D_{OV} = \frac{1+m}{2} + \frac{1-m}{2}\gamma_5 \mathrm{sgn}(H_M).$$

Möbius Domain Wall Fermions

- Möbius Domain wall fermions are defined by the choice of kernel operator

$$H_M = \frac{\gamma_5 D_w}{2 + \gamma_5 D_w}$$

in our effective 4D Overlap Operator

$$D_{4D} = \frac{1+m}{2} + \frac{1-m}{2}\gamma_5 \tanh[L_s \tanh^{-1}(H_M)].$$

- Approximation of the sign function using tanh with the Möbius domain wall fermion operator increases suppression of the Ginsparg Wilson violation to 0.14MeV.
- For this reason we are certain that simulation using the Möbius Domain Wall fermions provides an excellent symmetry with good control over artifacts which complicate analysis.

Symmetries of QCD from the Screening Mass of the 2-pt Correlation Function

Mesonic Correlators

- We consider the flavor triplet bilinear quark operators:

$$O(x) = \bar{q}(x)(\Gamma \otimes \frac{\vec{\tau}}{2})q(x).$$

  Here τ^a is an element of the generators of $SU(2)$.

- We measure the spatial correlator through:

$$C_\Gamma(z) = \int_{-\infty}^{\infty} dx \int_{-\infty}^{\infty} dy \int_0^\beta d\tau \, \langle O_\Gamma(z, x, y, \tau) O_\Gamma^\dagger(0) \rangle$$

  On the lattice this becomes

$$C_\Gamma(n_z) = \sum_{n_y, n_x, n_t} \langle O_\Gamma(n_z, n_x, n_y, n_t) O_\Gamma^\dagger(0, 0, 0, 0) \rangle \, .$$

Mesonic Spatial Correlators and Operators

Γ	Reference Name	Abbr.	Symmetry Correspondences	
$\mathbb{I}$	Scalar	S	$U(1)_A$	
γ_5	Psuedo Scalar	PS		
γ_1, γ_2	Vector	**V**	$SU(2)_L \times SU(2)_R$	$SU(2)_{CS}$?
$\gamma_1\gamma_5, \gamma_2\gamma_5$	Axial Vector	**A**		
$\gamma_0\gamma_3$	Tensor	$\mathbf{T}_t$	$U(1)_A$	
$\gamma_0\gamma_3\gamma_5$	Axial Tensor	$\mathbf{X}_t$		

- Due to rotational symmetries of the spatial correlator all data presented is based on an average of the correlation function over all spatial directions.

QCD Symmetries Revisited

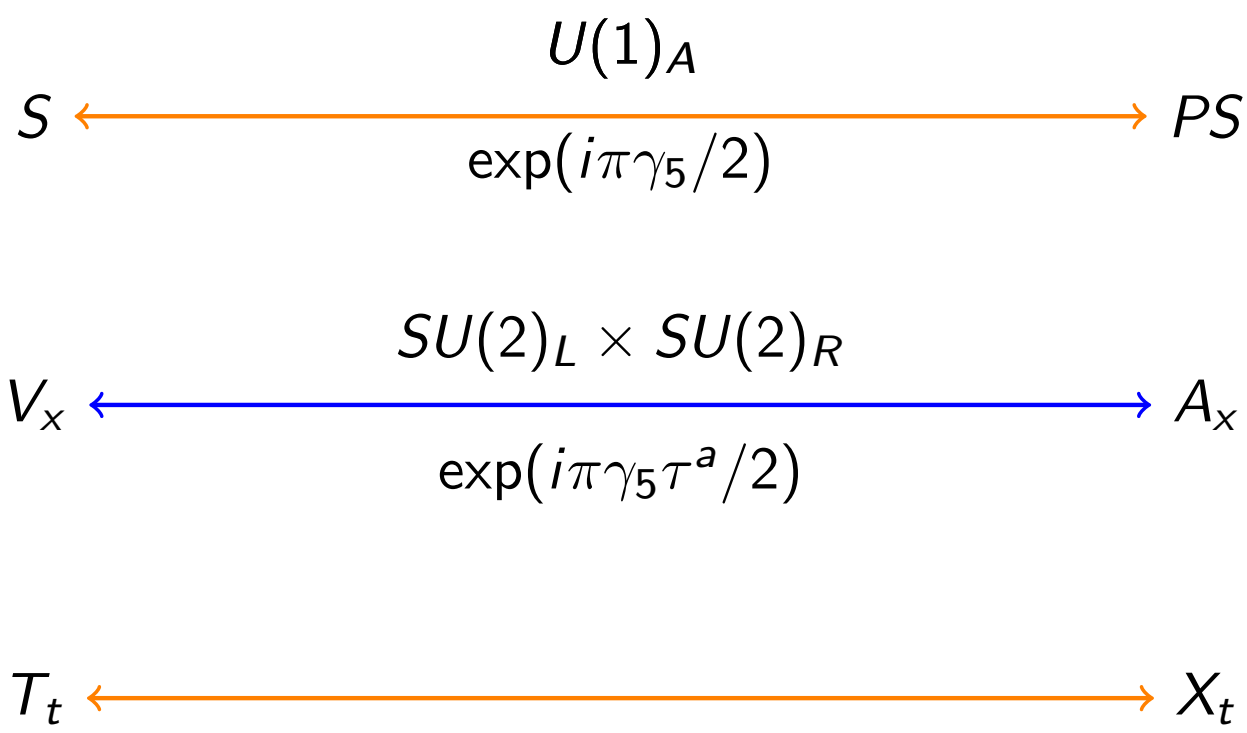

QCD Symmetries Revisited

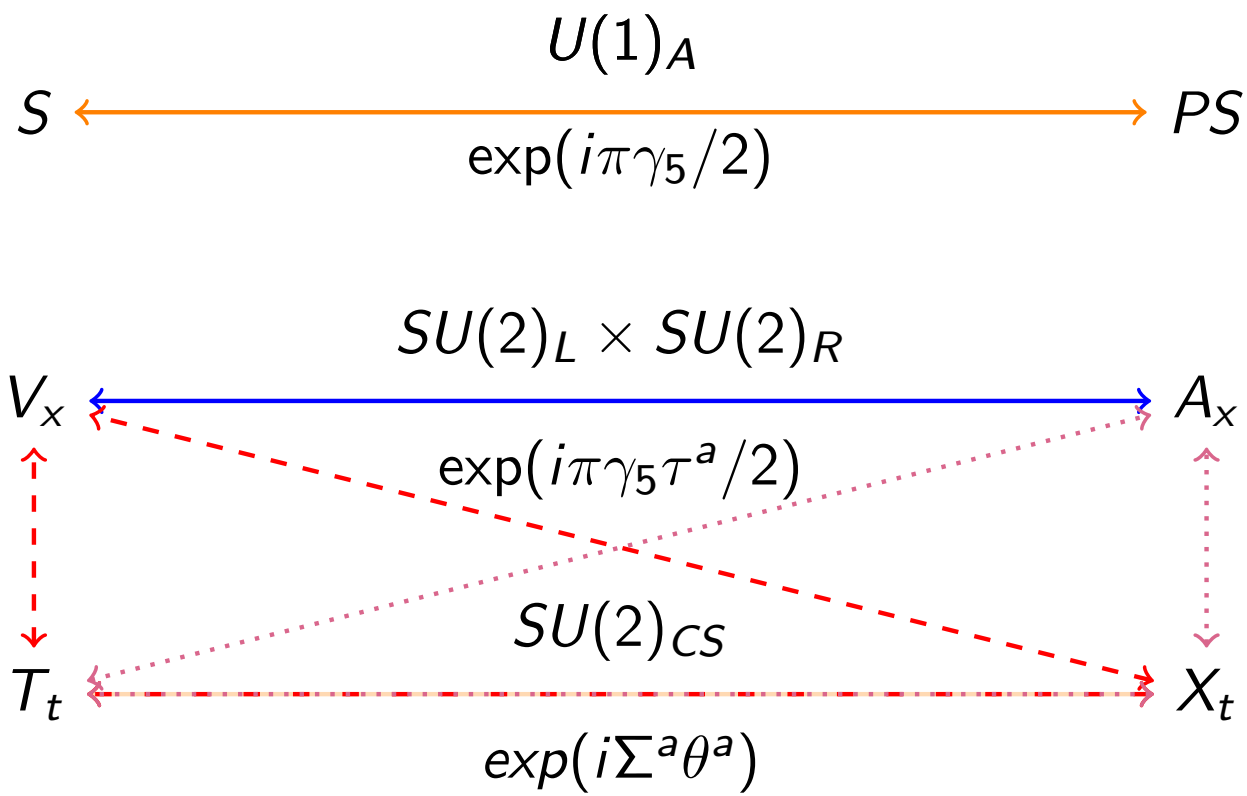

- Dashed and dotted lines represent respective isospin triplets related by $SU(2)_L \times SU(2)_R$ transformations.
- $SU(2)_{CS} \supset U(1)_A$

Effective Mass and Fit

- We use the $\cosh(z)$ fitting ansatz.
- Symmetries examined from the difference in the screening masses between channels related by associated transformations. i.e.

$$\text{For } SU(2)_L \times SU(2)_R: \quad \Delta M = |m_{fit}^{Ax} - m_{fit}^{Vx}|$$

$$\text{For } U(1)_A: \quad \Delta M = |m_{fit}^{PS} - m_{fit}^{S}|$$
$$\Delta M = |m_{fit}^{Xt} - m_{fit}^{Tt}|$$

$$\text{For } SU(2)_{CS}: \quad \Delta M = |m_{fit}^{Ax} - m_{fit}^{Xt}|$$

Numerical Analysis

Fixed β Simulation Parameters

- $N_f = 2$ QCD with Möbius domain wall fermions and Symanzick gauge action.
- $L_s = 16$
- $a^{-1} = 2.643\text{GeV}$
- $L = 32 - 48$ $(2.40 - 3.60fm)$
- m_{ud} from $\sim 2.6\text{MeV}$ to 13.2MeV(covering $m_{phys} \sim 4\text{MeV}$)
- Temperature ranges from $T = 146MeV - 330\text{MeV}$.
- psuedo $T_c \sim 165\text{MeV}$ estimated by chiral susceptibility

$L^3 \times L_t$	β	$T[MeV]$	am	$m[MeV]$
$36^3 \times 18$	4.30	146	0.0010	2.6
			0.0050	13.2
$48^3 \times 18$	4.30	146	0.0010	2.6
			0.0050	13.2
$32^3 \times 16$	4.30	165	0.0010	2.6
			0.0050	13.2
$40^3 \times 16$	4.30	165	0.0010	2.6
			0.0050	13.2
$32^3 \times 14$	4.30	190	0.0010	2.6
			0.0050	13.2
$24^3 \times 12$	4.30	220	0.0010	2.6
			0.0050	13.2
$32^3 \times 12$	4.30	220	0.0010	2.6
			0.0050	13.2
$40^3 \times 12$	4.30	220	0.0050	13.2
$48^3 \times 12$	4.30	220	0.0010	2.6
			0.0050	13.2
$32^3 \times 10$	4.30	264	0.0050	13.2
$32^3 \times 8$	4.30	330	0.0010	2.6
			0.0050	13.2

Line of Constant Physics Simulation Parameters

- $N_f = 2 + 1$ QCD with Möbius domain wall fermions.
- $L_s = 12$
- $L = 36$
  $a^{-1} = 1.562 - 2.453\text{GeV}$,
  $L = 48$ $a^{-1} = 2.211 - 4.001\text{GeV}$
- $L = 36$ $(2.89 - 4.54fm)$
  $L = 48$ $(2.37 - 4.27fm)$
- m_{ud} remains approximately chiral throughout the range with $m_{ud} \approx m_s/27$
- Temperature ranges from $T = 130\text{MeV} - 250\text{MeV}$.
- psuedo $T_c \sim 156\text{MeV}$

$L^3 \times L_t$	β	$T[MeV]$	am	$m[MeV]$
$36^3 \times 12$	4.02	130	-0.003341	-5.22
	4.04	139	-0.001656	-2.78
	4.05	145	-0.001079	-1.87
	4.06	150	-0.000611	-1.10
	4.07	155	-0.000244	-0.453
	4.08	160	0.000053	0.101
	4.09	164	0.000293	0.578
	4.11	174	0.000602	1.26
	4.17	204	0.001001	2.46
$48^3 \times 16$	4.13	138	0.000805	1.78
	4.15	146	0.000930	2.17
	4.17	153	0.001001	2.46
	4.18	157	0.001022	2.57
	4.20	165	0.001041	2.74
	4.23	176	0.001033	2.92
	4.30	205	0.000939	3.07
	4.405	250	0.000760	3.04

Effective Mass and Fit Range – $U(1)_A$

S

PS

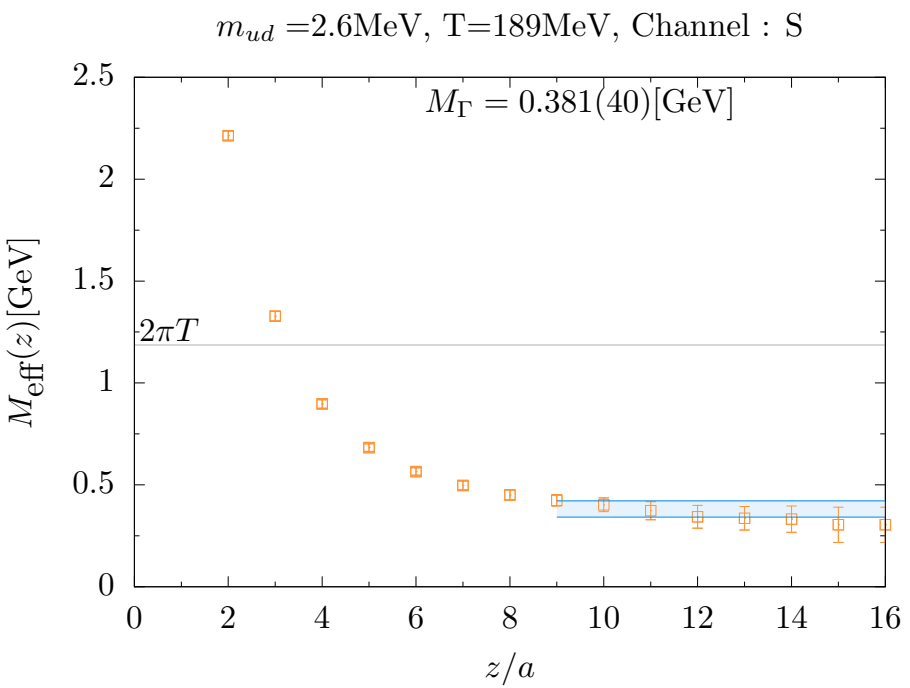

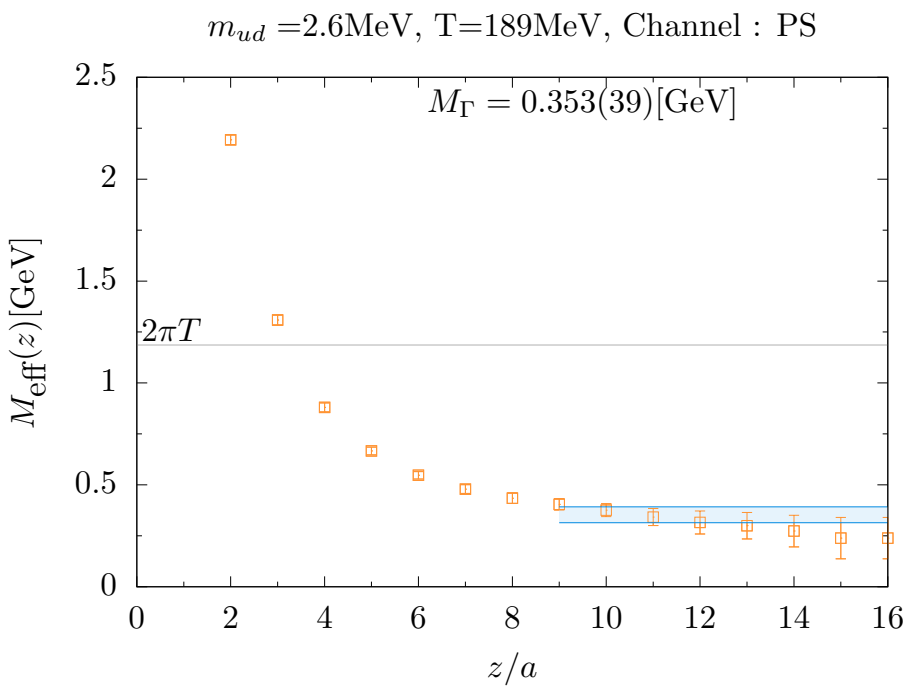

$T = 189$MeV at $m_{ud} = 2.6$MeV

Effective Mass and Fit Range – $U(1)_A$

T_t X_t

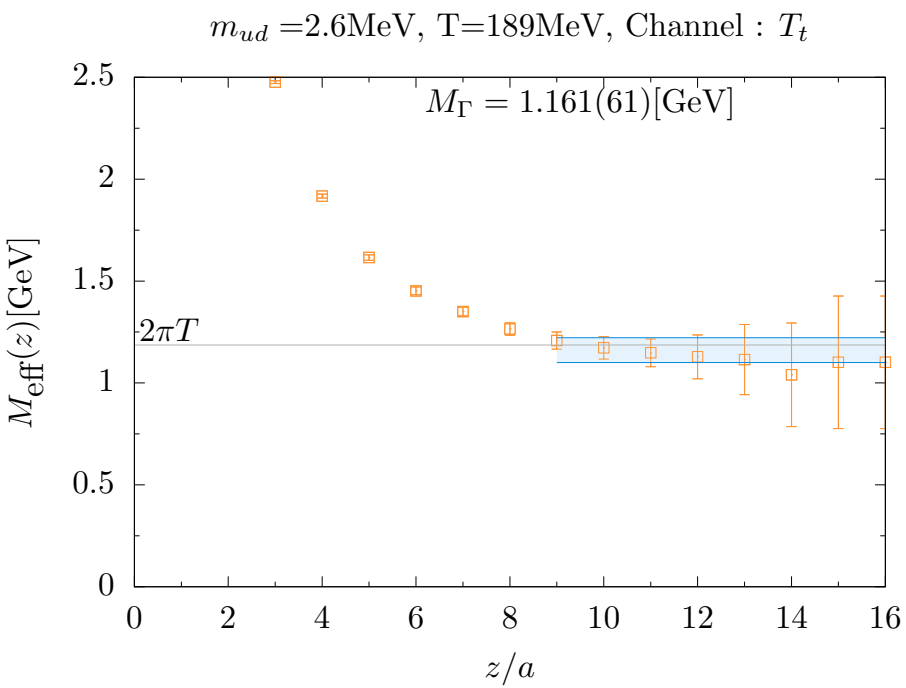

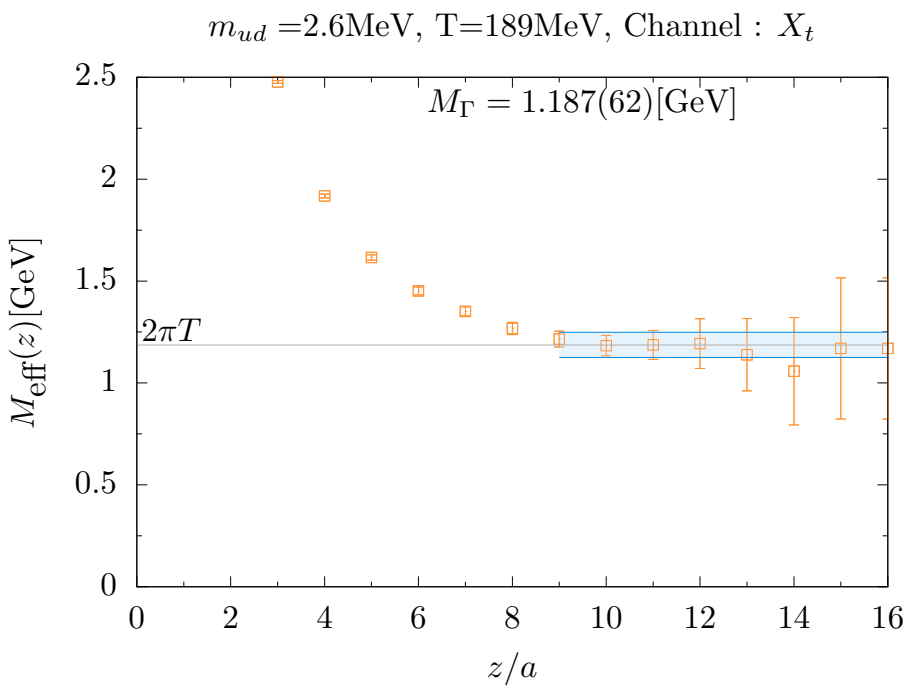

$T = 189$MeV at $m_{ud} = 2.6$MeV

Effective Mass and Fit Range – $SU(2)_L \times SU(2)_R$

A_x V_x

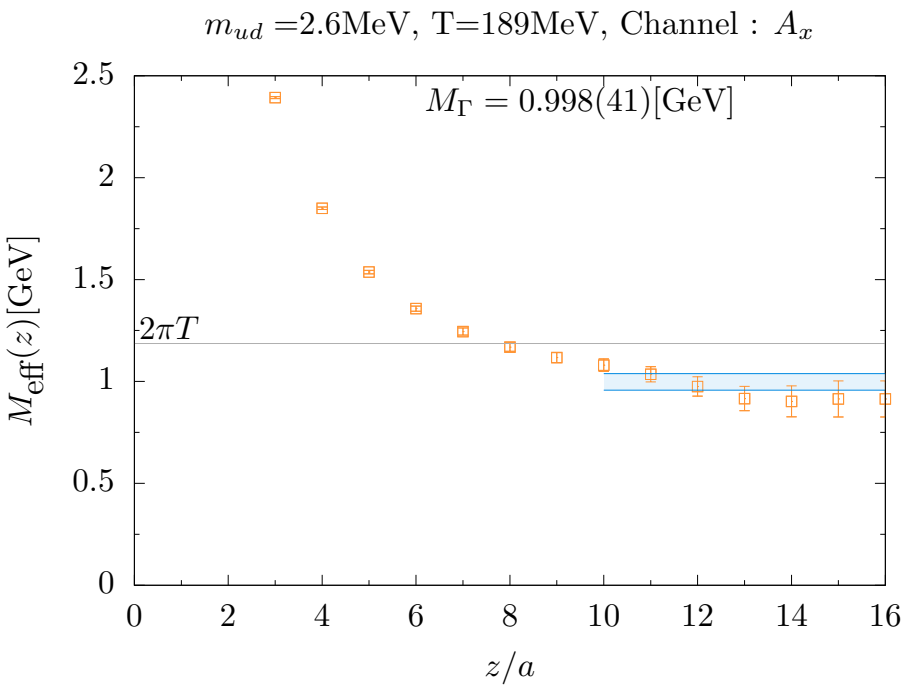

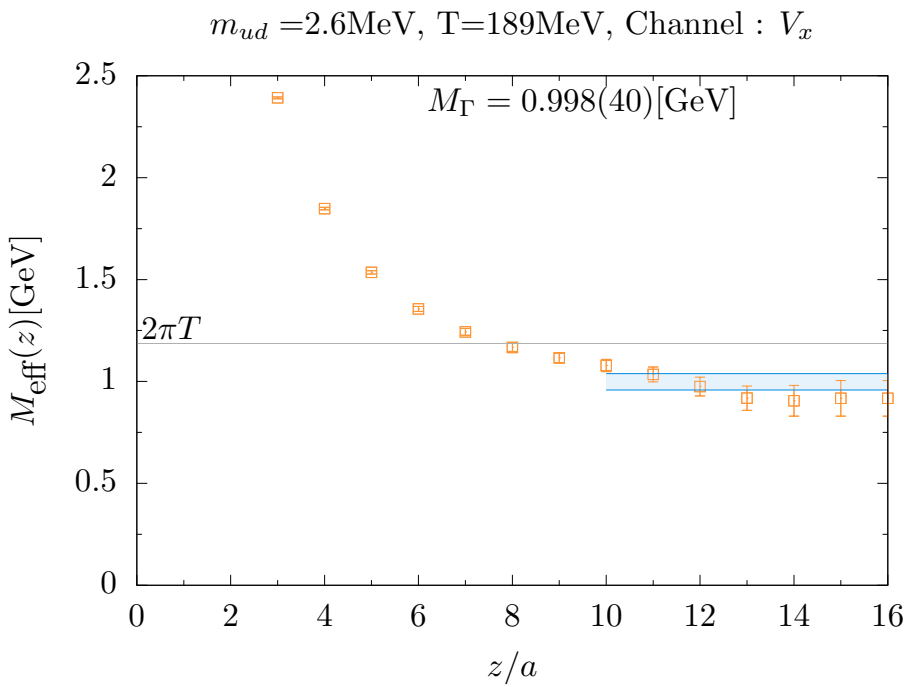

$T = 189$MeV at $m_{ud} = 2.6$MeV

Correlator Channel Temperature Spectrum

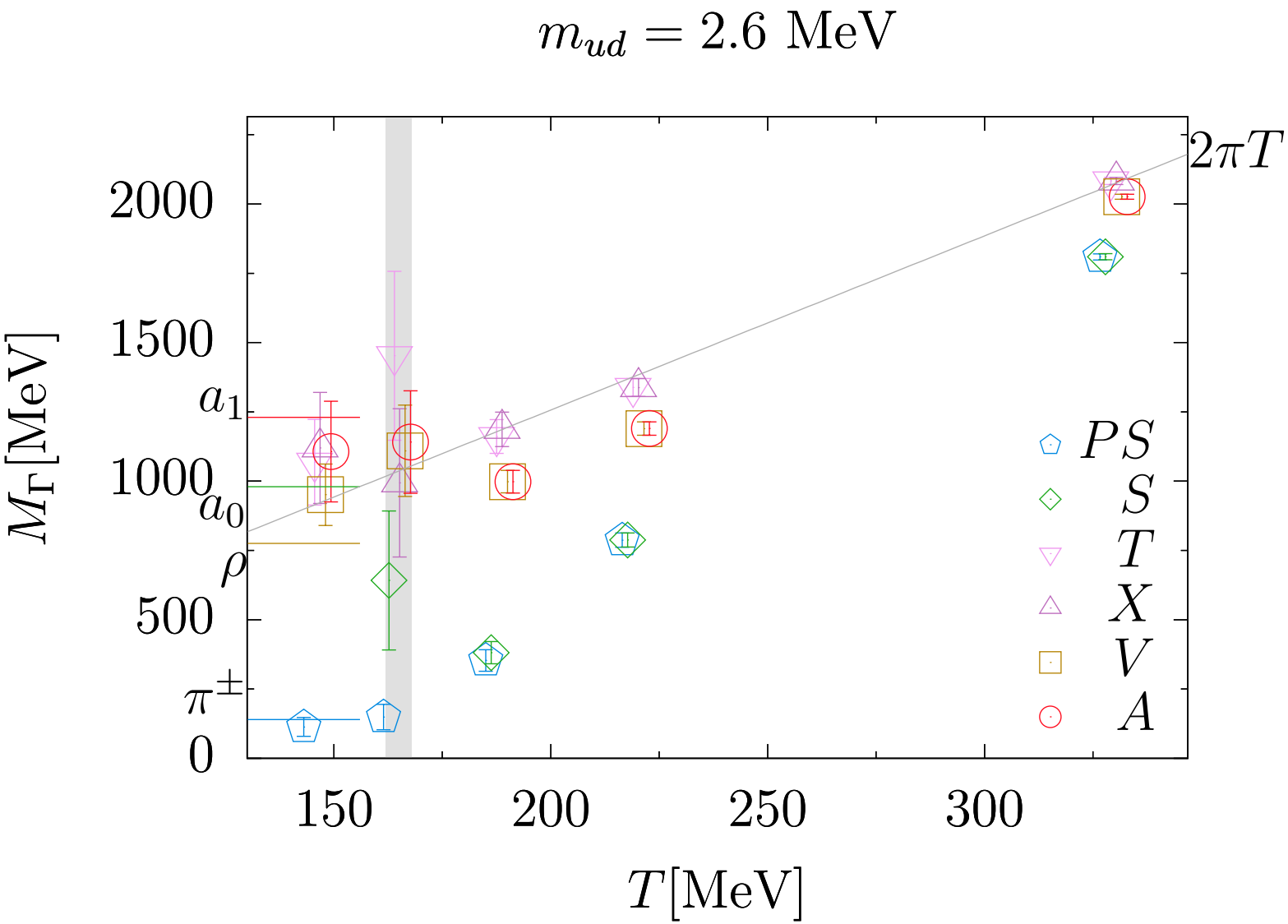

Correlator Channel Temperature Spectrum

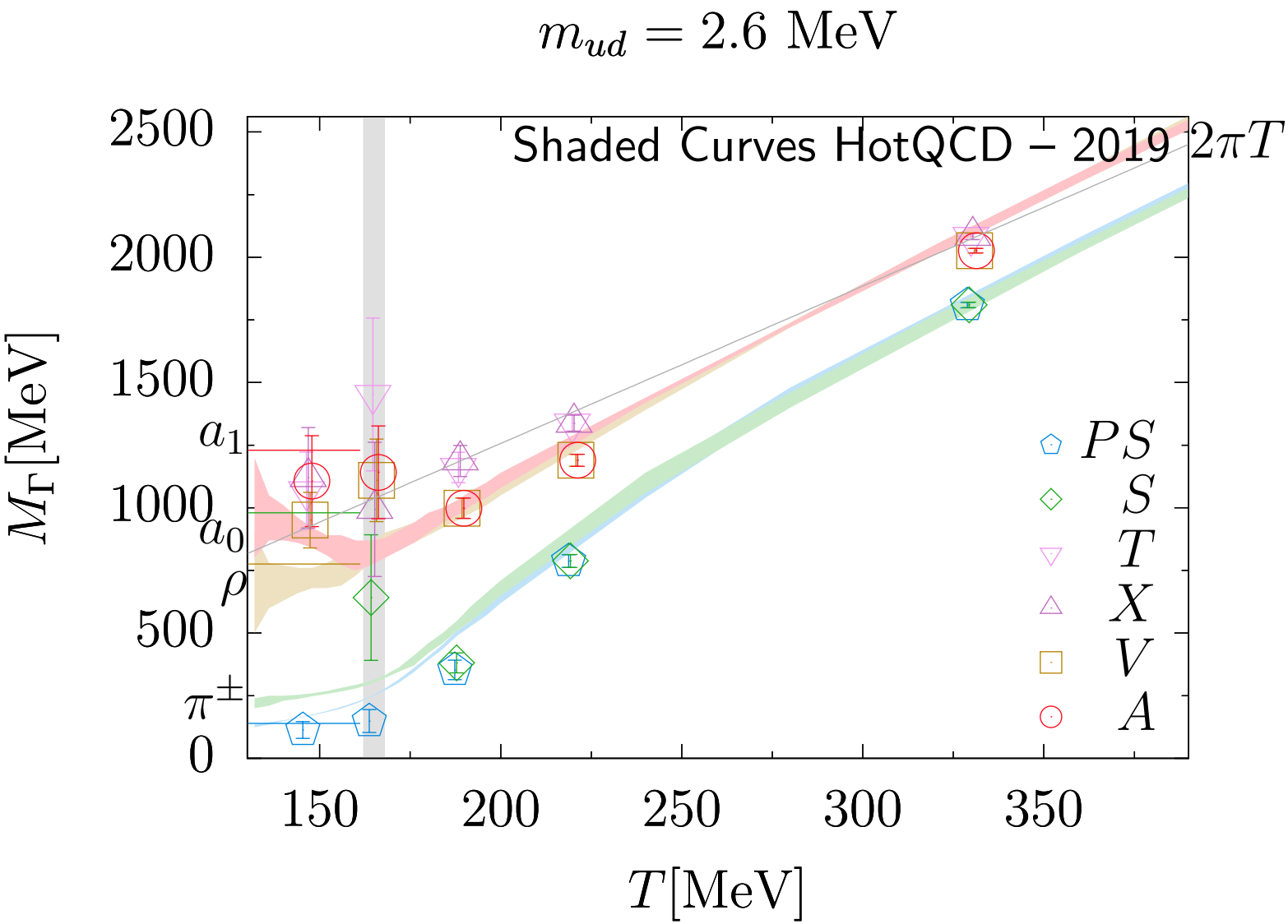

Correlator Channel Temperature Spectrum

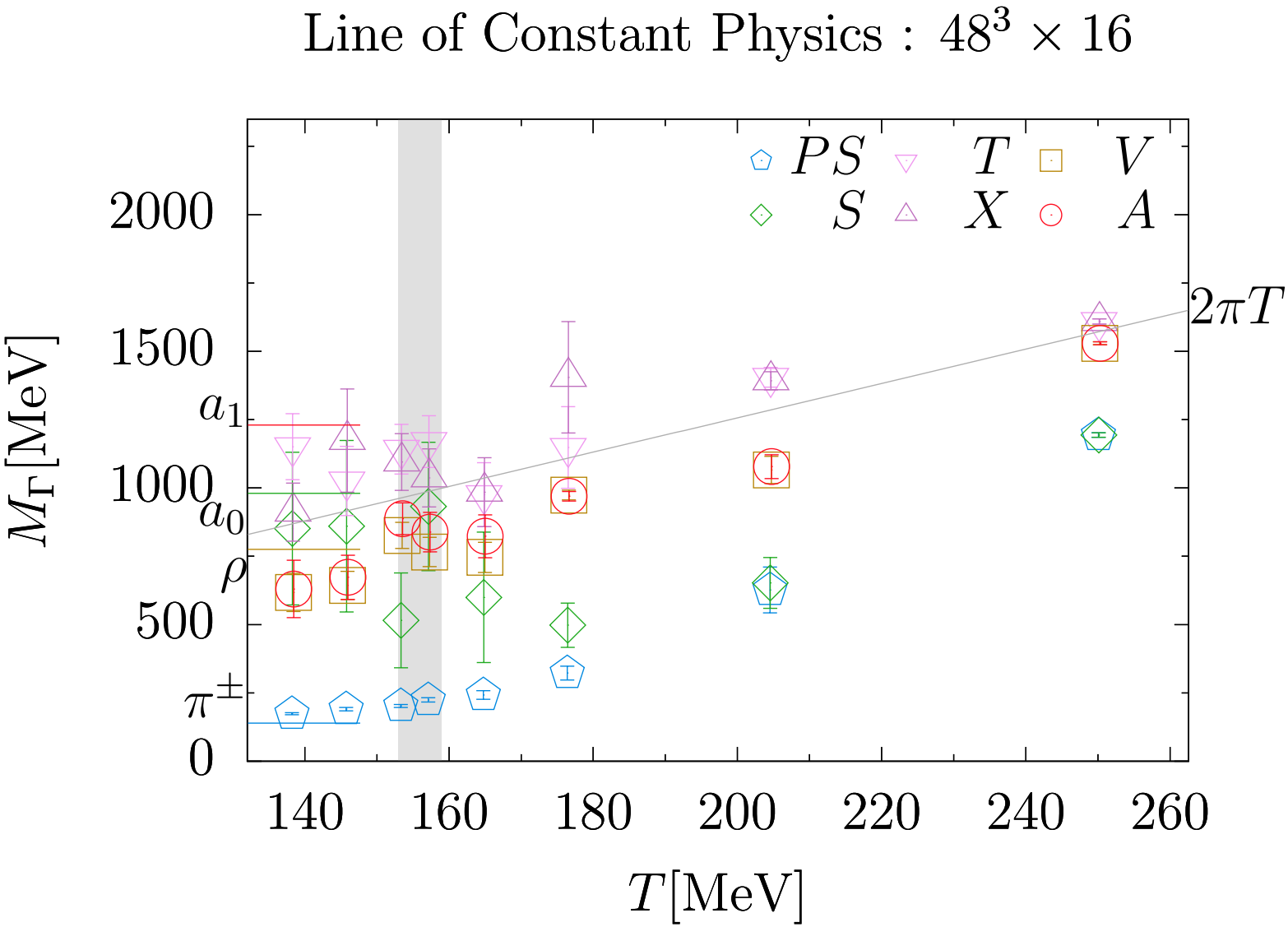

Normalized Correlator Channel Temperature Spectrum

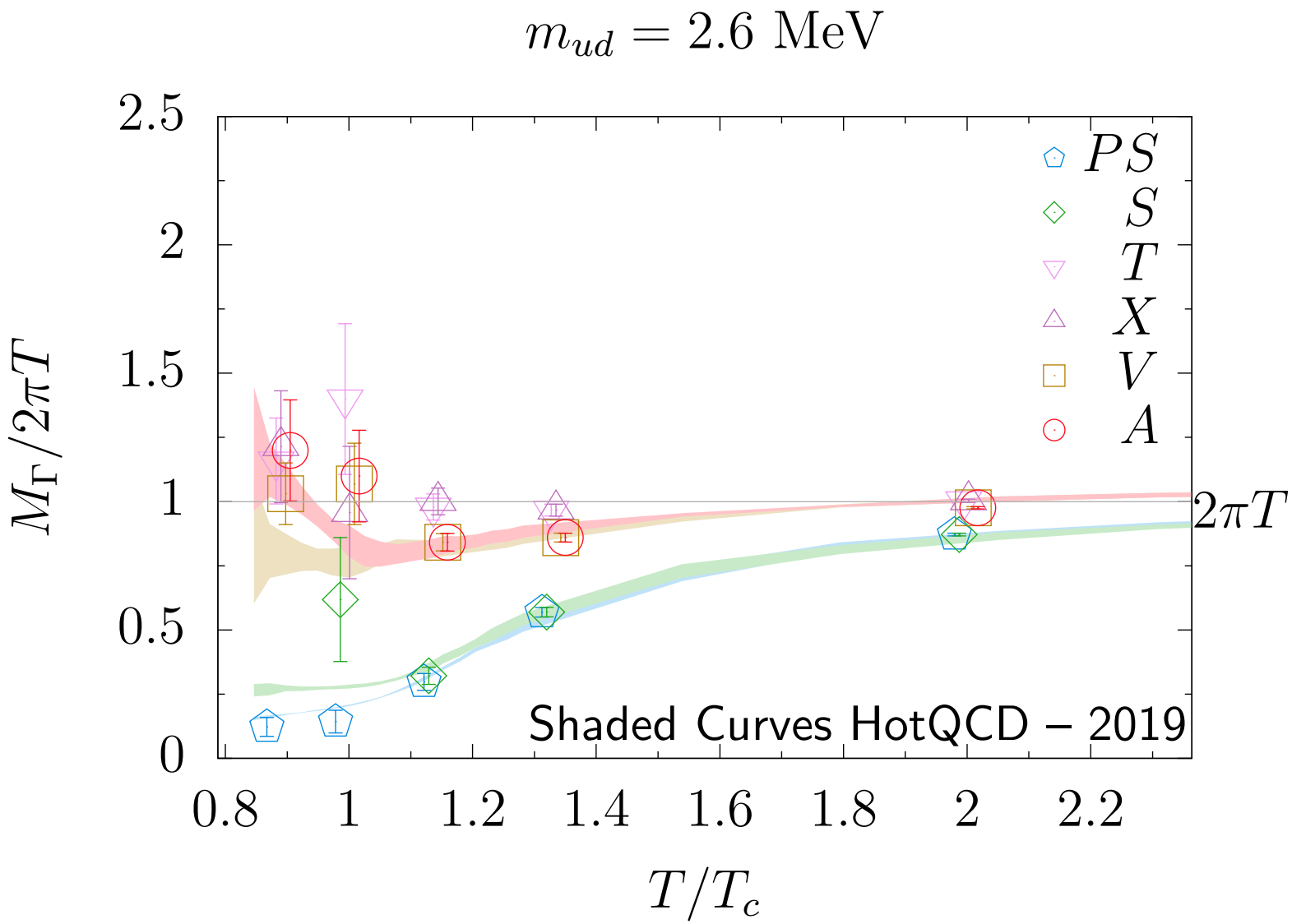

Normalized Correlator Channel Temperature Spectrum

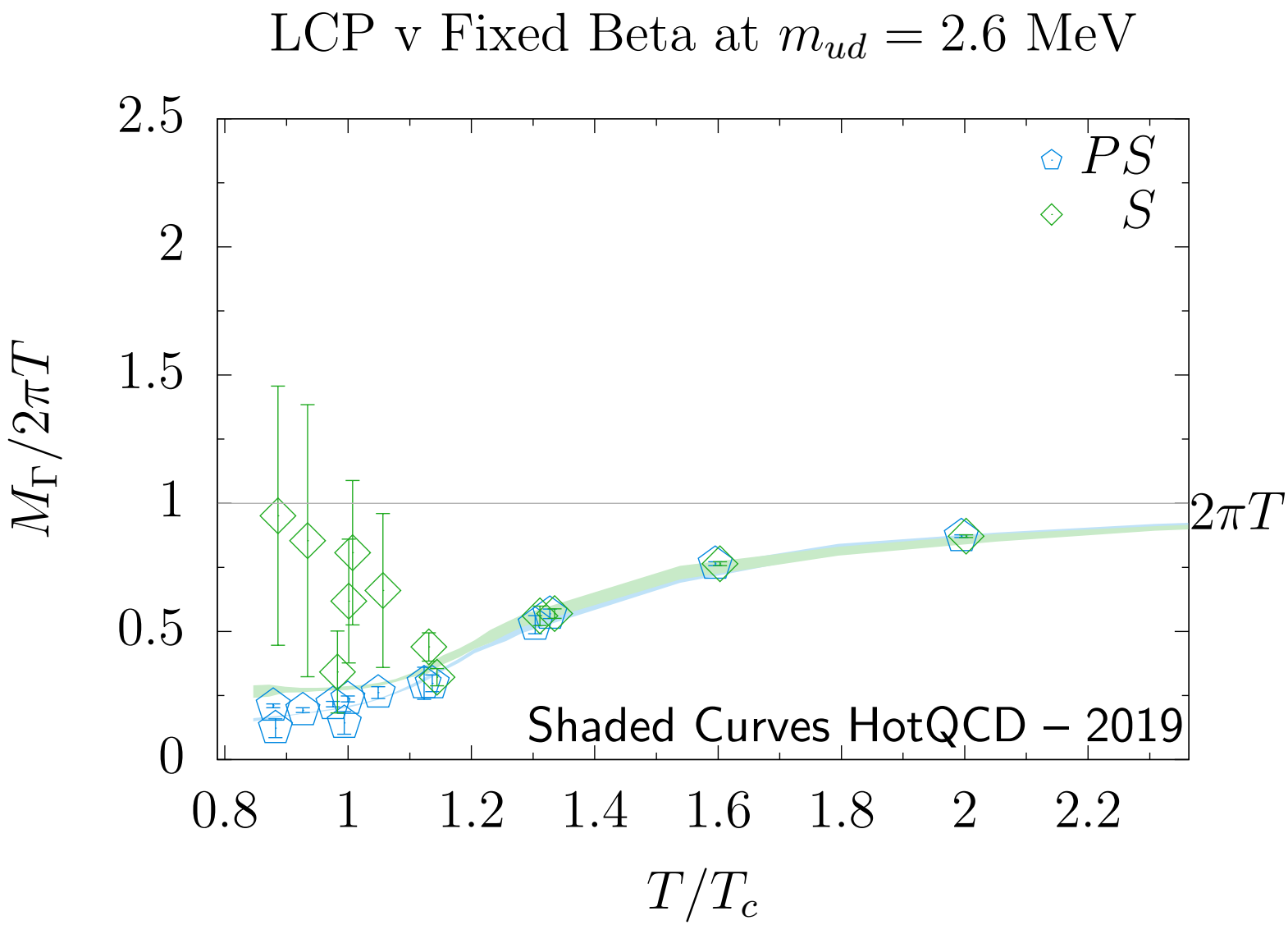

Normalized Correlator Channel Temperature Spectrum

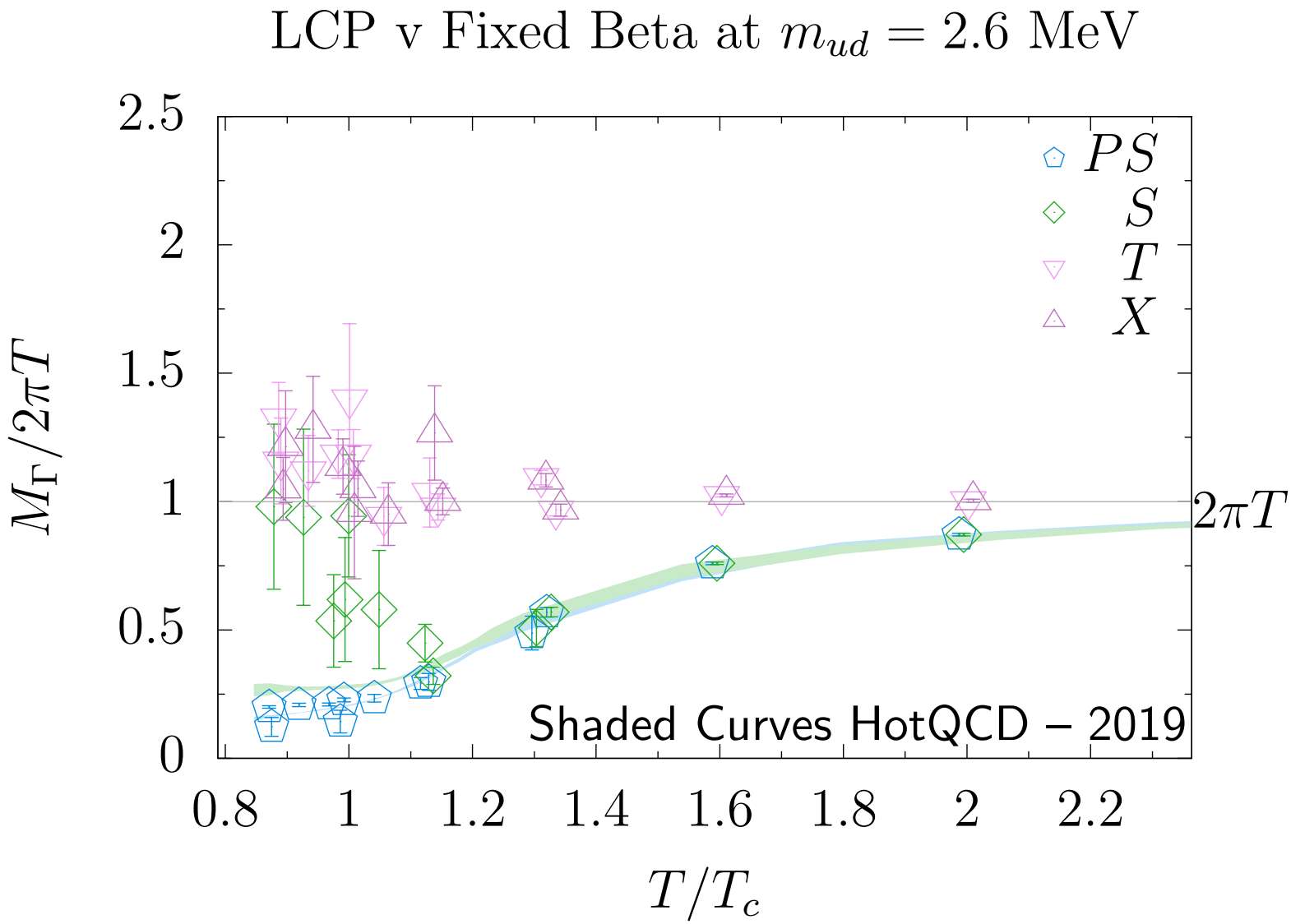

Normalized Correlator Channel Temperature Spectrum

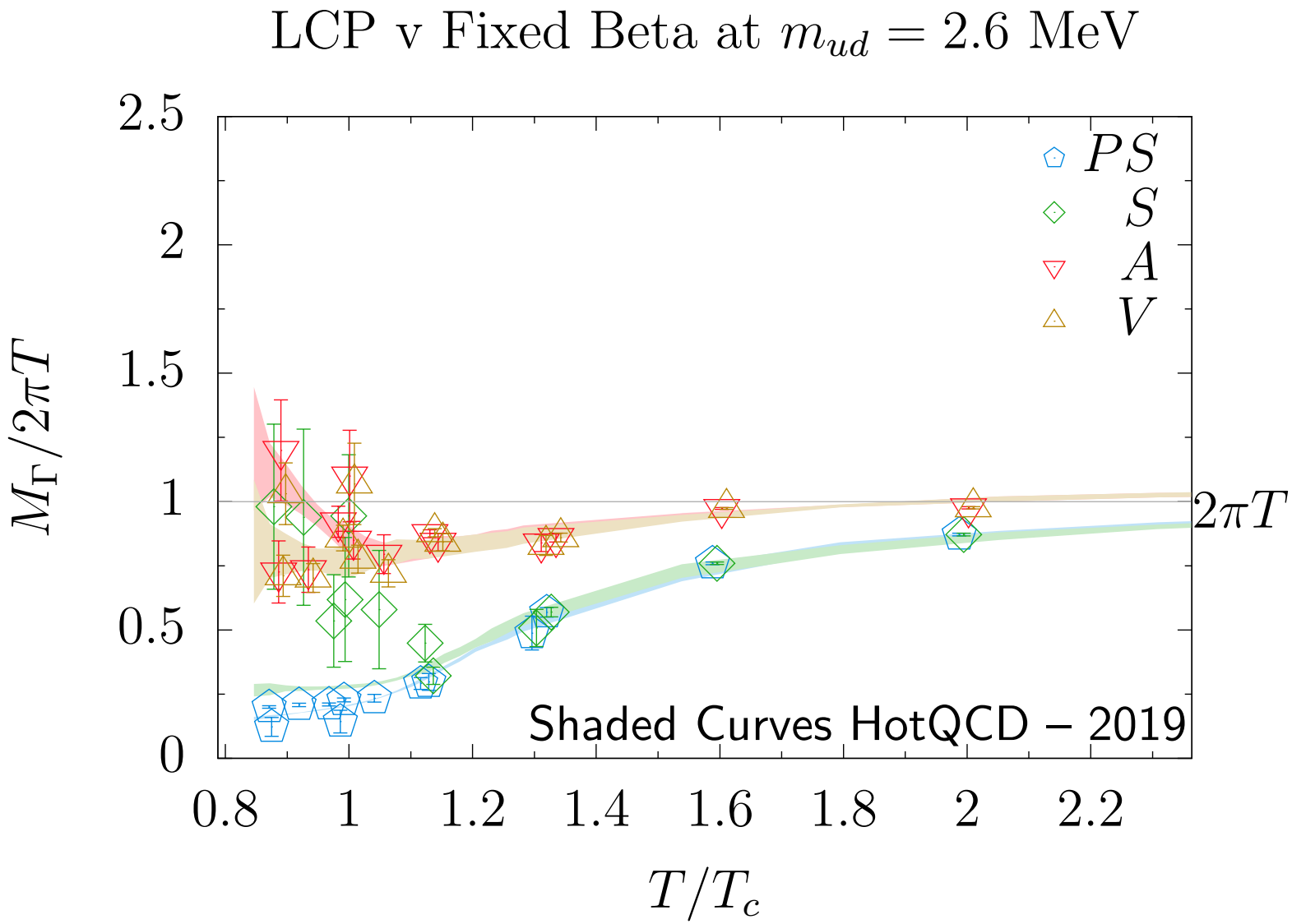

Normalized Correlator Channel Temperature Spectrum

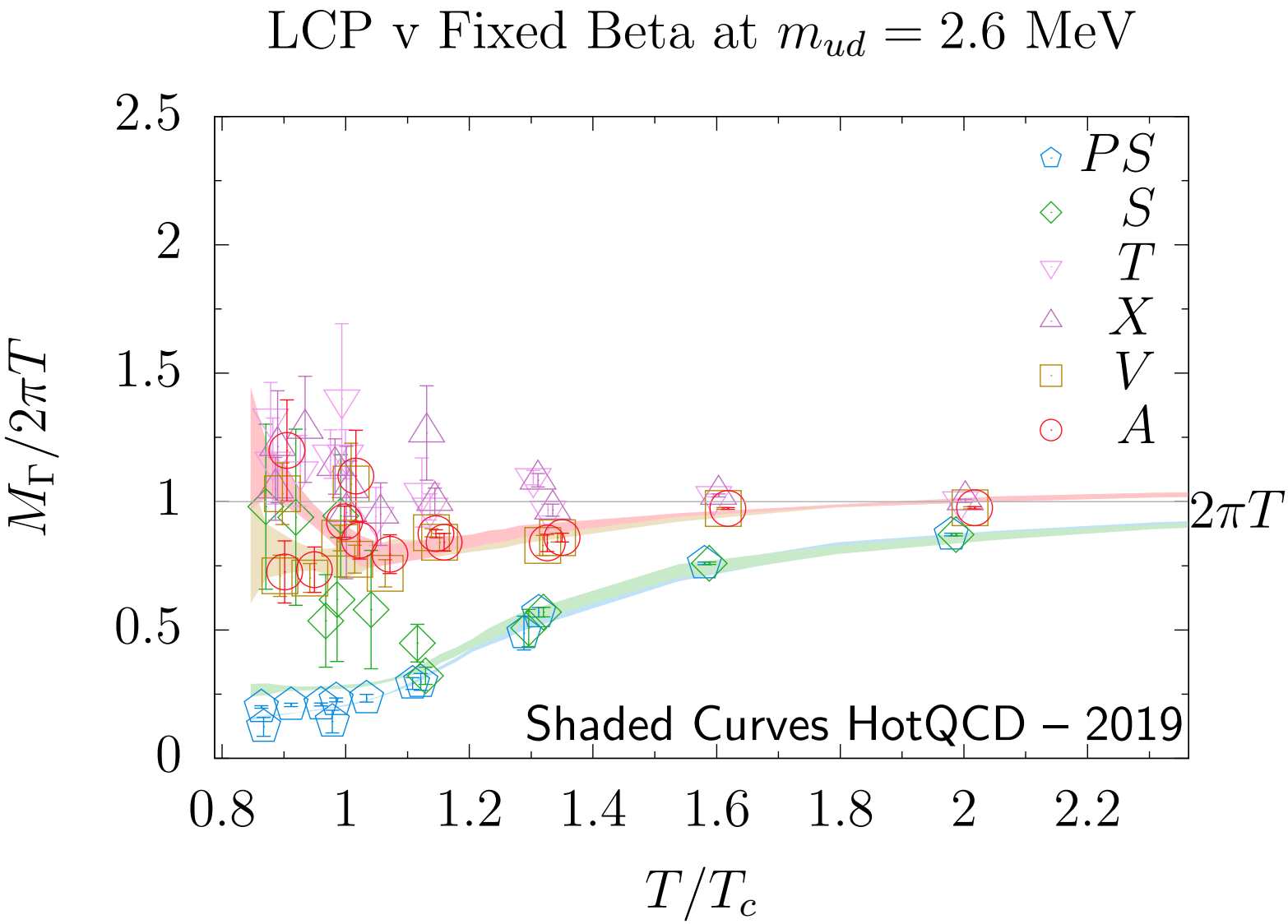

2πT convergence

- For the temperature dependent screening mass it is predicted that the high temperature limit of the spectrum tends toward the perturbative correction [1],

$$\frac{M_\Gamma}{2\pi T} = 1 + Cg^2 + \mathcal{O}(g^4) \approx 1 + 0.02980106477g^2.$$

- The strongest characteristics of the leading contribution are seen in the heaviest X_t and T_t channels which converge very quickly to $2\pi T$ above T_c.
- Next to leading order is not approachable from these studies.
- This suggests that the high temperature limit is potentially more symmetric [11, 12, 13, 14].

[1] Laine and Vepsalainen . *JHEP.* **02**. P. 004. 2004 [arXiv:hep-ph/0311268]
[11, 12, 13, 14] Glozman . *Acta Phys. Polon. Supp.* **10**. P. 583. 2017 [arXiv:1610.00275], Glozman . *Eur. Phys. J. A.* **54**. P. 117. 2018 [arXiv:1712.05168], Catillo . *Int. J. Mod. Phys. A.* **37**. P. 2250102. 2022 [arXiv:2109.03532], Glozman, Philipsen, and Pisarski . *Eur. Phys. J. A.* **58**. P. 247. 2022 [arXiv:2204.05083]

Correlator Channel Temperature Spectrum and Symmetry

- While high temperature features for the $48^3 \times 16$ lattice appear to be consistent with the continuum extrapolation, at low temperatures the curves are noisy and inconsistent with the behavior seen in the $N_f = 2$ study.
- This is worse for the $36^3 \times 12$ lattice and suggests we may have lattices which are too coarse in the low temperature limit.
- Any study of the symmetry from these lattices, therefore, are not considered reliable.
- The Line of Constant Physics study by JLQCD remains ongoing, hopefully we will see improved analysis by Lattice 2027.

$SU(2)_L \times SU(2)_R$ symmetry

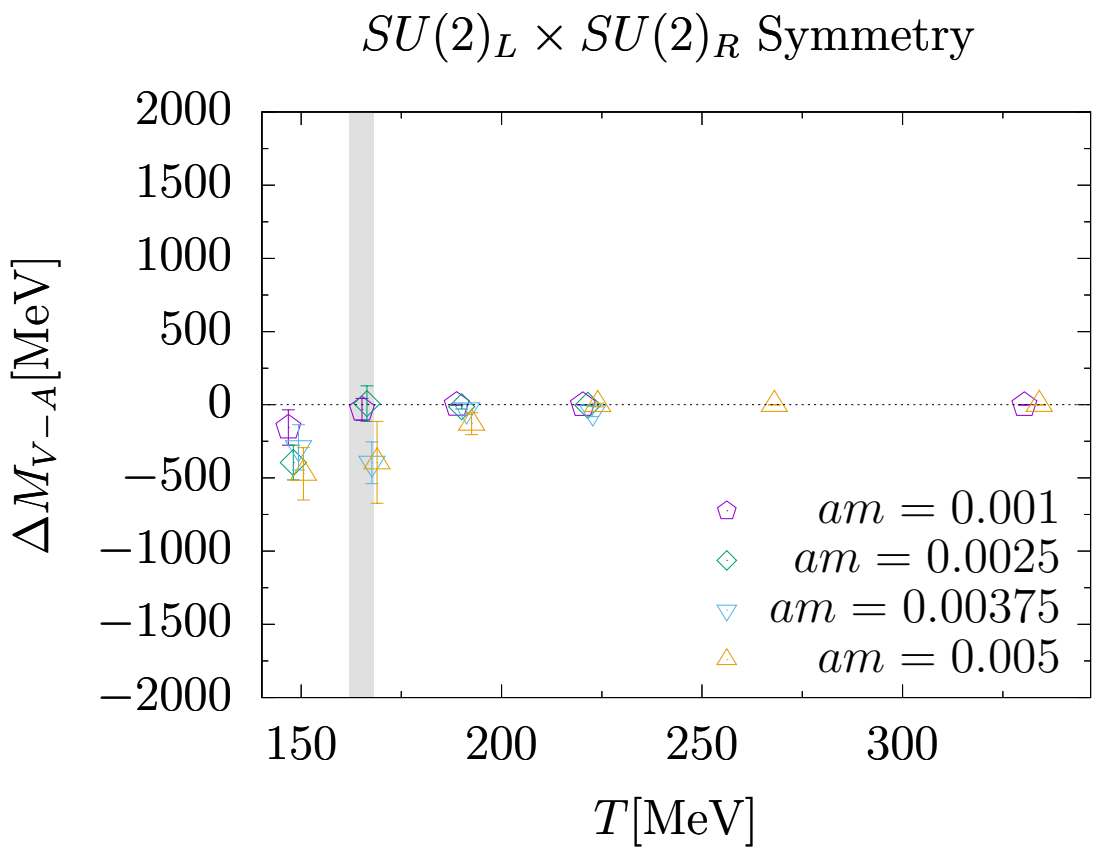

- At $T \sim 165$MeV restoration of $SU(2)_L \times SU(2)_R$ show the same characteristic behaviors for 2.6MeV and 6.6MeV near the physical $m_{ud} \sim 4$MeV.

$SU(2)_L \times SU(2)_R$ symmetry

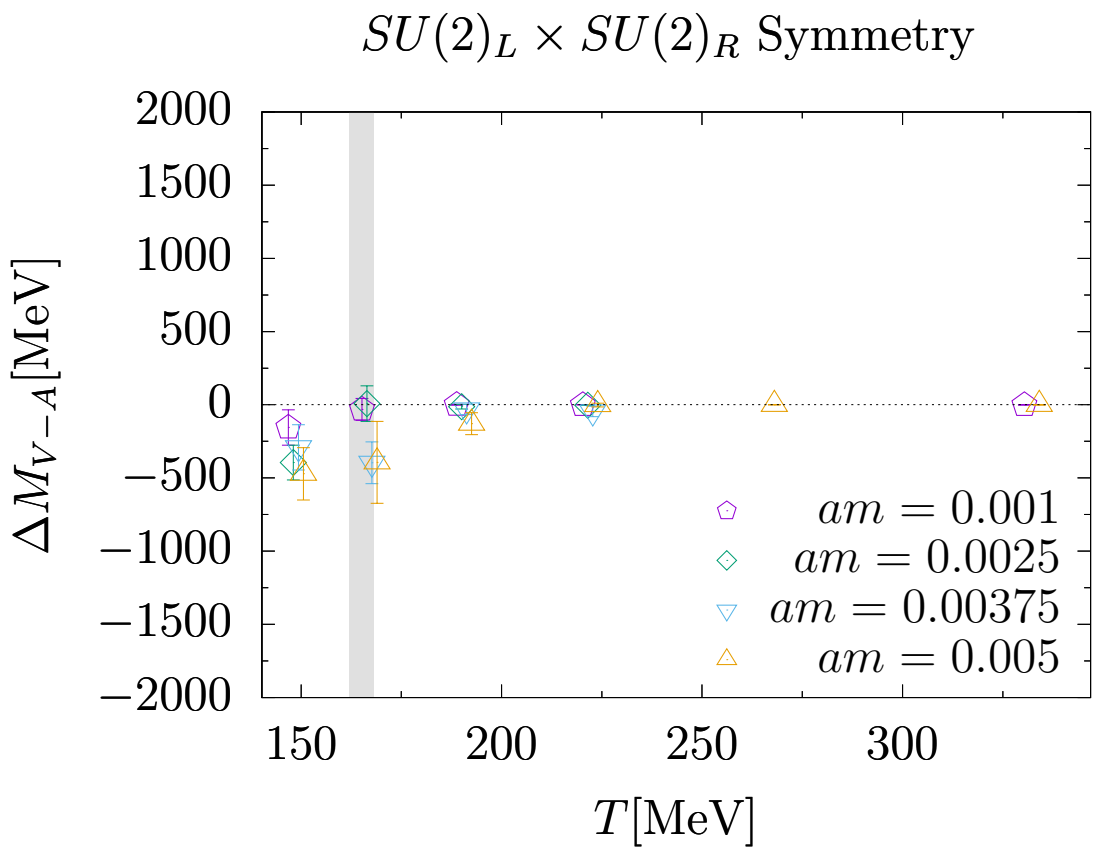

- $|M_V - M_A|/M_A \sim 2.8\%$ at $T = 165$MeV and 0% from 189-330MeV.

$U(1)_A$ symmetry through $Xt - Tt$

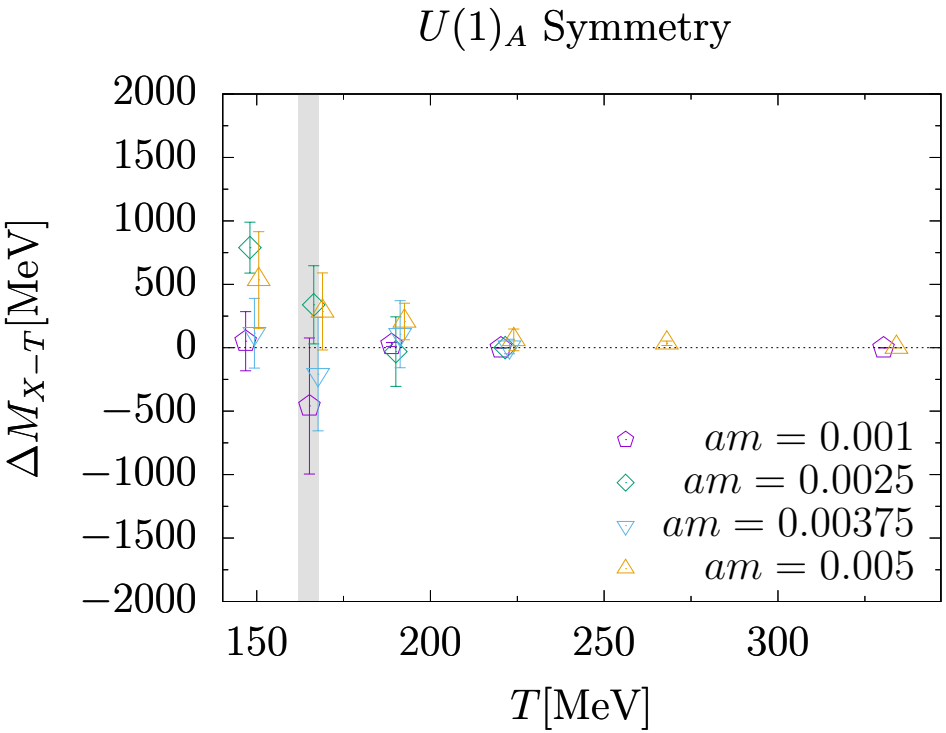

- The anomaly appears to be strongly suppressed for $T \sim T_c$.
- Crucially, $|M_{X_t} - M_{T_t}|/M_{T_t} \sim 32(36)\%$ at $T = 165$MeV and reduces to $2(1)\%$ at $T = 189$MeV.

$U(1)_A$ symmetry through $PS - S$

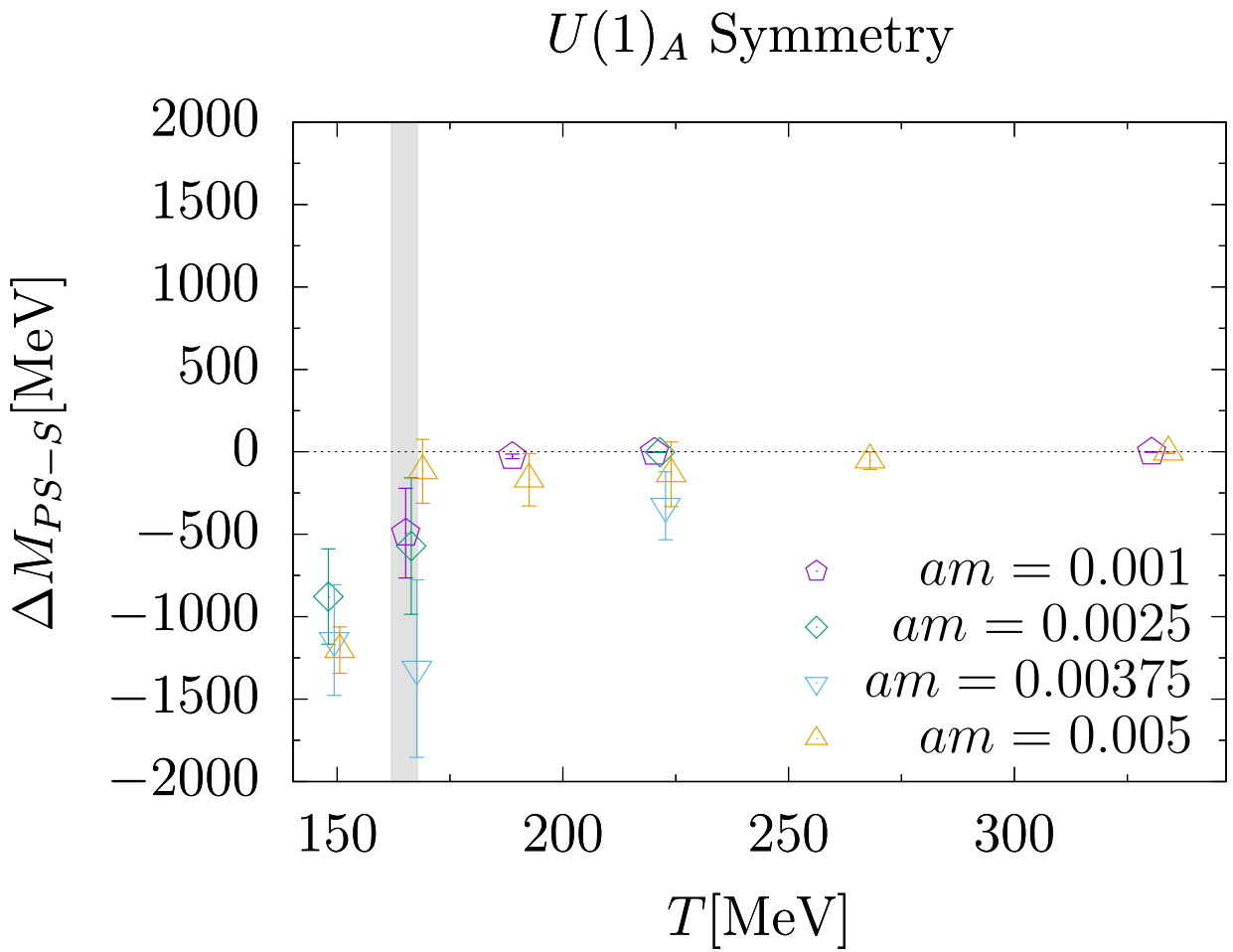

- $PS - S$ shows the same behaviors as $Xt - Tt$ and mirrors behaviors in $SU(2)_L \times SU(2)_R$ but is significantly noisier due to scalar channel noise.

$U(1)_A$ symmetry through $PS - S$

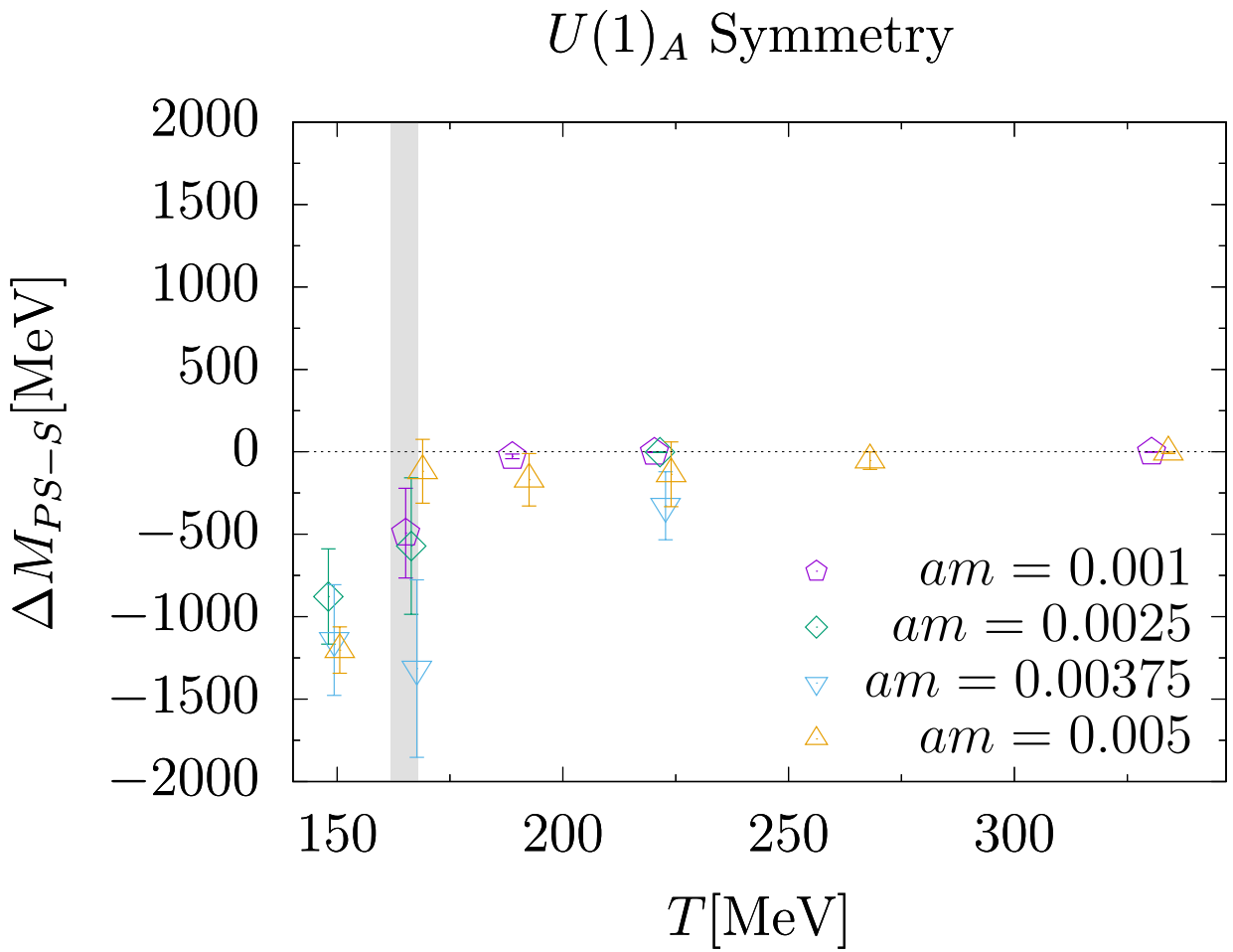

- $|M_{PS} - M_S|/M_S \sim 77(42)\%$ at T_c however, at $T = 189$MeV $|M_{PS} - M_S|/M_S \sim 7(4)\%$.

$SU(2)_{CS}$ symmetry

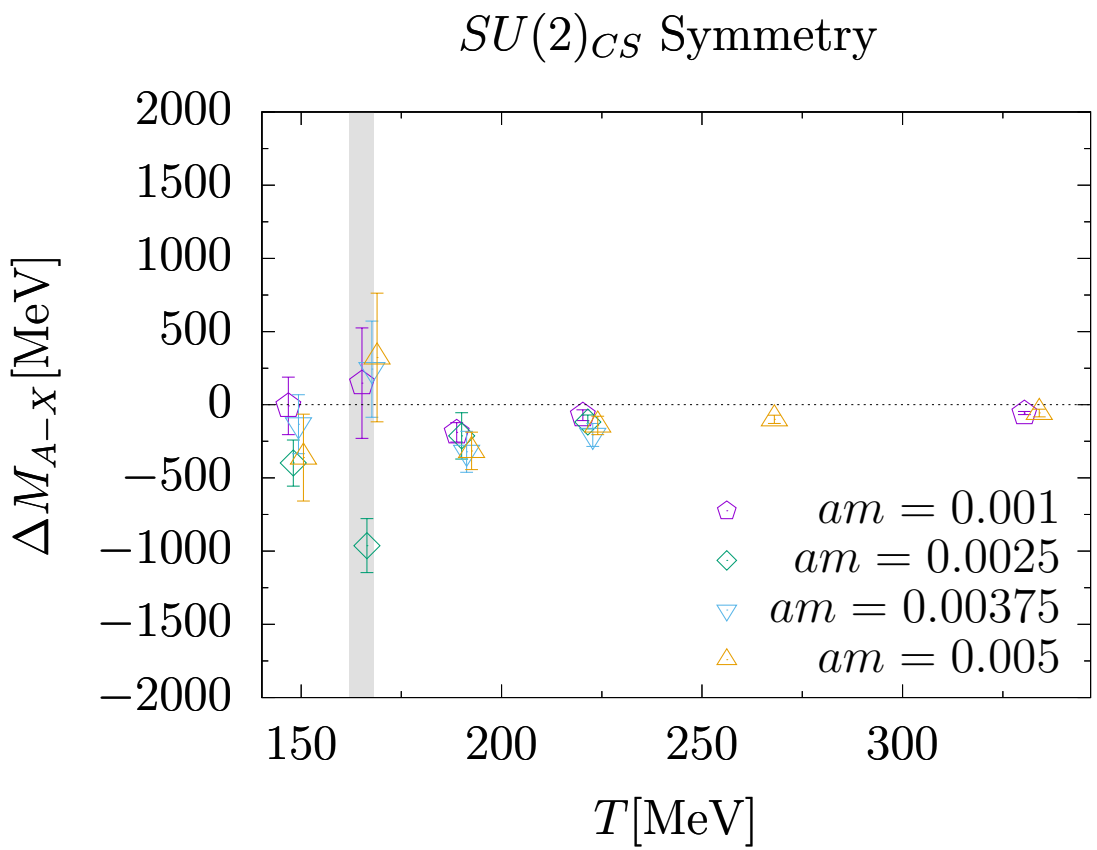

- At $2T_c$ $T = 330$MeV, $|\Delta M_{A-\chi_t}|/T \sim 17(3)\%$, which is still large.

$SU(2)_{CS}$ symmetry

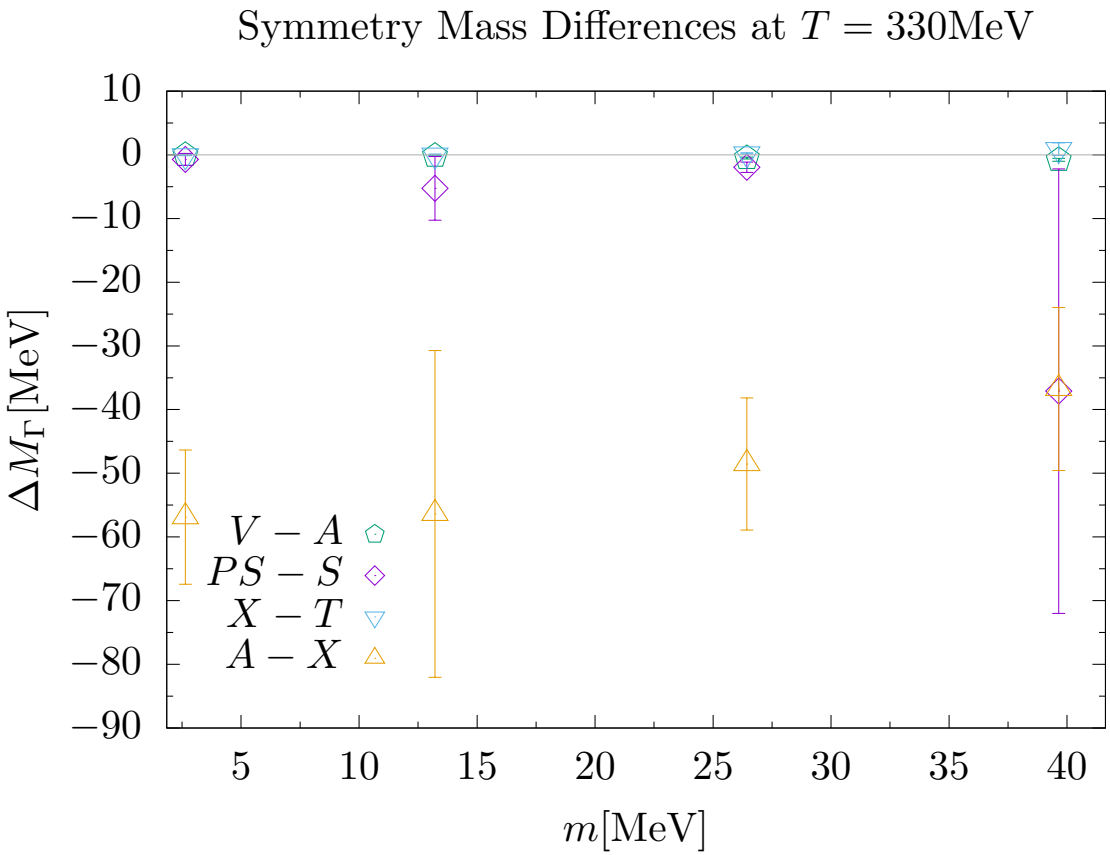

- At $2T_c$ $T = 330$MeV, $|\Delta M_{A-X_t}|/T \sim 17(3)\%$, which is still large.

$SU(2)_{CS}$ symmetry

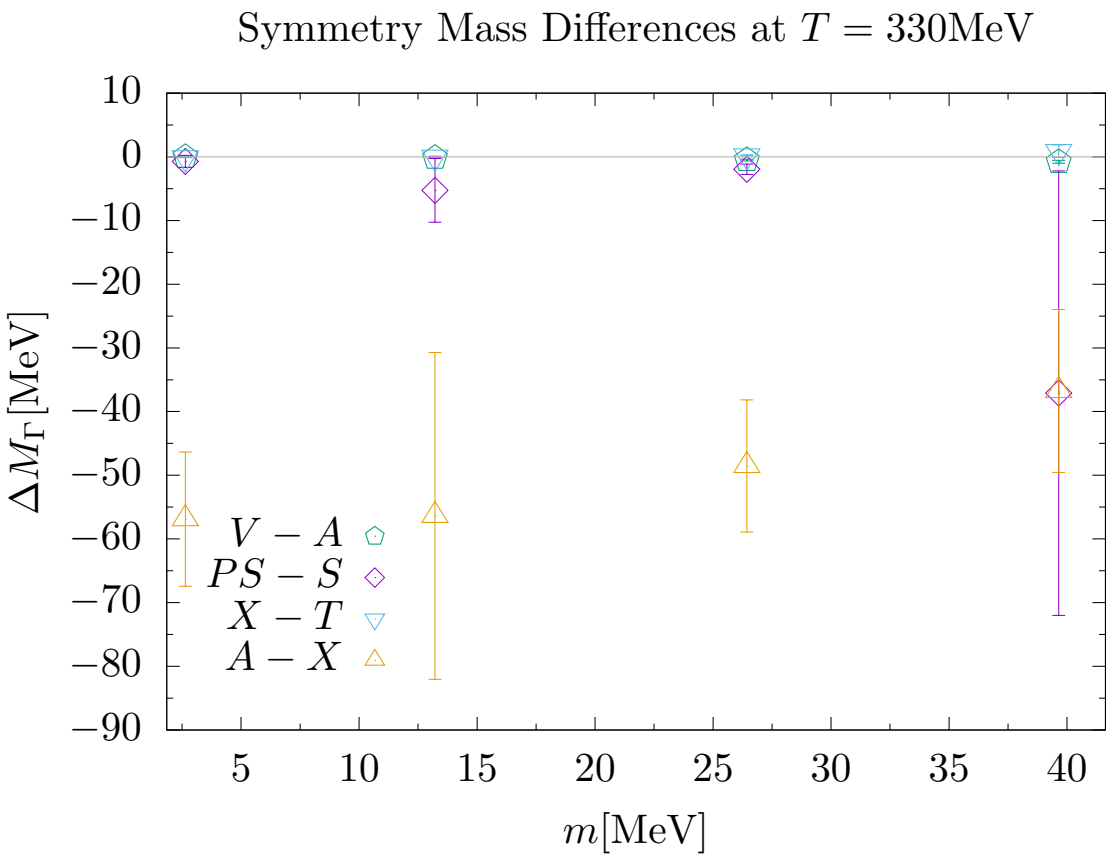

- Potentially at higher temperatures an emergence of $SU(2)_{CS}$ may occur.

Systematic error analysis

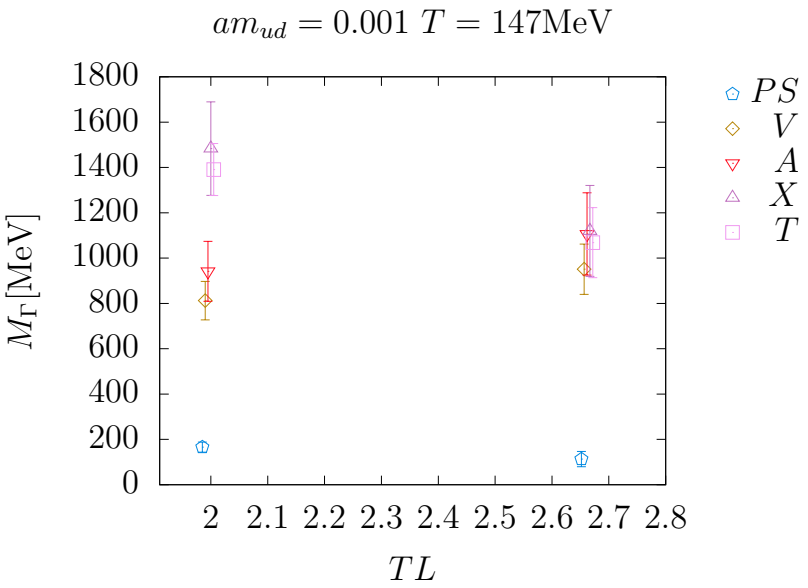

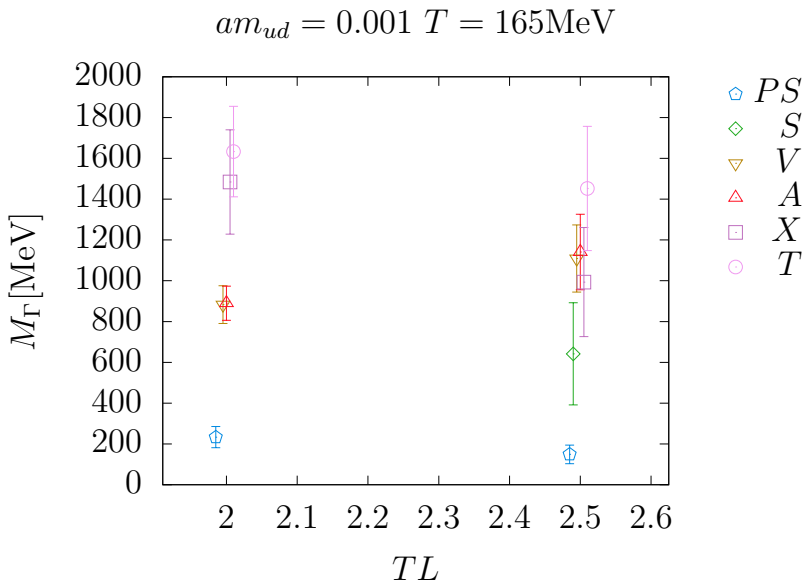

- Finite volume effects are overlapping within 1σ.
- For this study we simulated lattice with a single spacing 0.075fm only.
- Our estimation for discretization error in symmetry 5.4×10^{-5} from (am_{res}), estimation of error in the correlator 3.9×10^{-3} from $(aT_c)^2$.

Conclusion

Summary

- We have quantitatively examined various symmetries of QCD at temperatures $[0.9, 2]\,T_c$.
- Möbius Domain Wall fermions offer a good chiral symmetry with mild violation of the Ginsparg-Wilson relation.
- Using the mesons screening mass extracted from the cosh fit we looked at the temperature dependence of six isovector channels.
- For fixed beta $N_f = 2$, $0.9\,T_c$ and T_c we simulated two lattice volumes as a control on finite volume effects.
- For LCP we studied the same range across two volumes 36 and 48.
- For all lattices in our study we simulated masses in the range $2.6 - 13.2$MeV, covering the physical point.

Conlusion

- We find the screening masses are consistent with the $T = 0$ experimental values of the meson spectrum already at $0.9\,T_c$ for $m = 0.0010$.
- Conversely, at high temperatures the screening mass approaches $2\pi T$.
- ΔM_{V-A} indicates restoration of $SU(2)_L \times SU(2)_R$ at $T_c \sim 165\text{MeV}$.
- $\Delta M_{T_t - X_t}$ and ΔM_{PS-S} show an analogous behavior for $U(1)_A$, indicating suppression of the anomaly close to, if not at, T_c.
- Our probe for $SU(2)_{CS}$ is $\Delta M_{A-X_t} \sim 50\text{MeV}$ at $T = 2T_c$ and may be only approximate.
- For the LCP study we found that the finer lattices (with correspondingly larger β) will offer a better signal for study of chiral symmetry, and future finer lattices show promise for an equivalent $N_f = 2 + 1$ to the fixed beta $N_f = 2$ data.

Thank you

Backup Slides

Screening Mass – Cosh Ansatz

- Generically we can decompose the spatial correlator into a spectrum of screening mass states

$$C(z) = A_0 e^{-M_0 z} + A_1 e^{-M_1 z} + \ldots,$$

  at long range, the lightest screening mass will dominate the correlator signal.
- For a periodic lattice we can assume at long ranges around the middle of the lattice there are two long range screening masses

$$C(z) = A_0 e^{-M_0 z} + A_0 e^{-M_0 (N_z - z)}.$$

- For a periodic lattice symmetric around the midpoint we can approximate the correlator as cosh like

$$C(z) = A_0' \cosh[M_0 (z - N_z/2)].$$

Effective Mass and Fit Range – $U(1)_A$ – LCP

S

PS

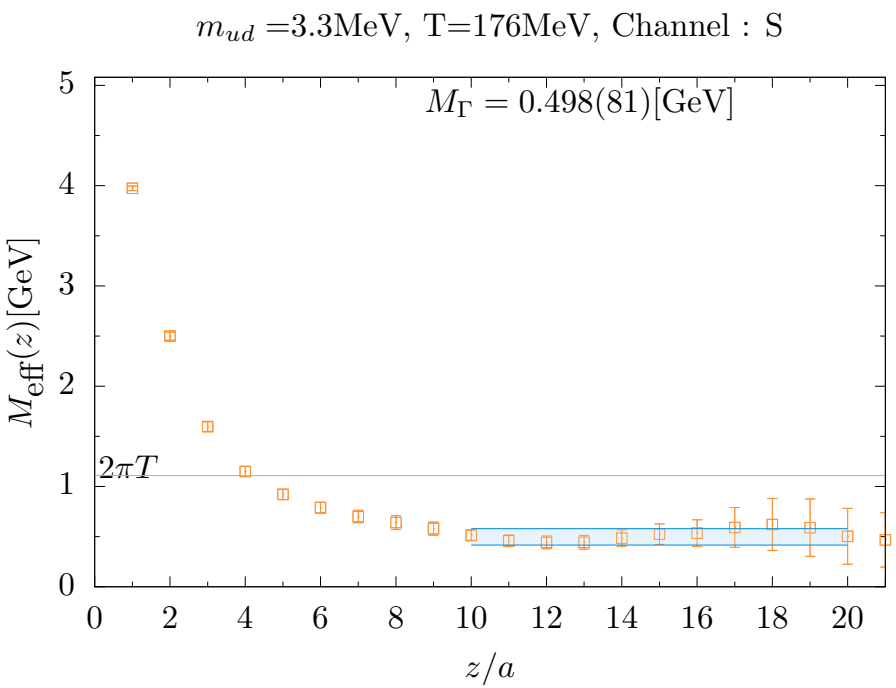

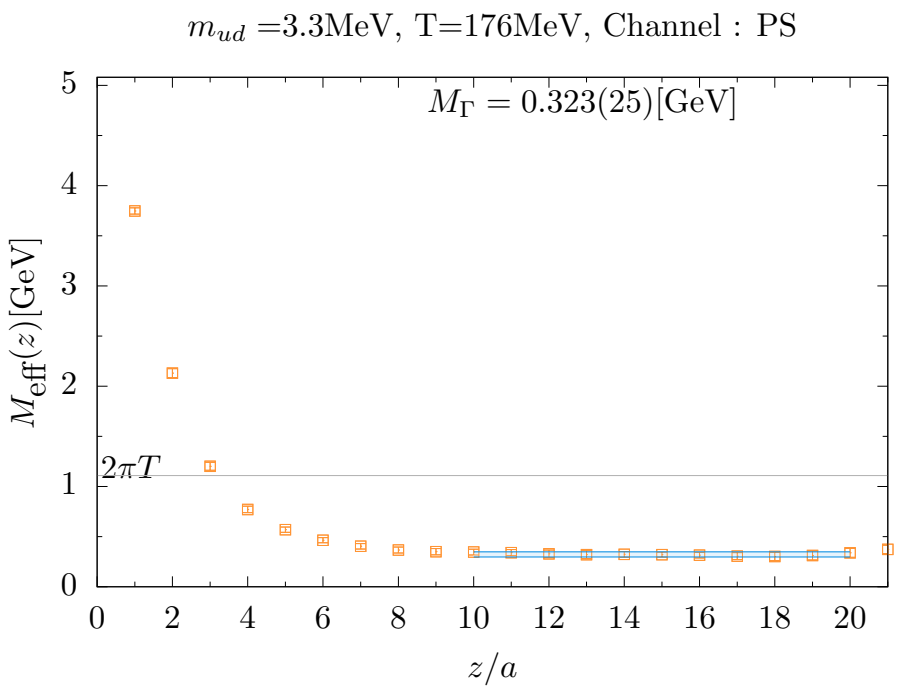

$T = 176$MeV at $m_{ud} = 2.92$MeV

Effective Mass and Fit Range – $U(1)_A$ – LCP

T_t X_t

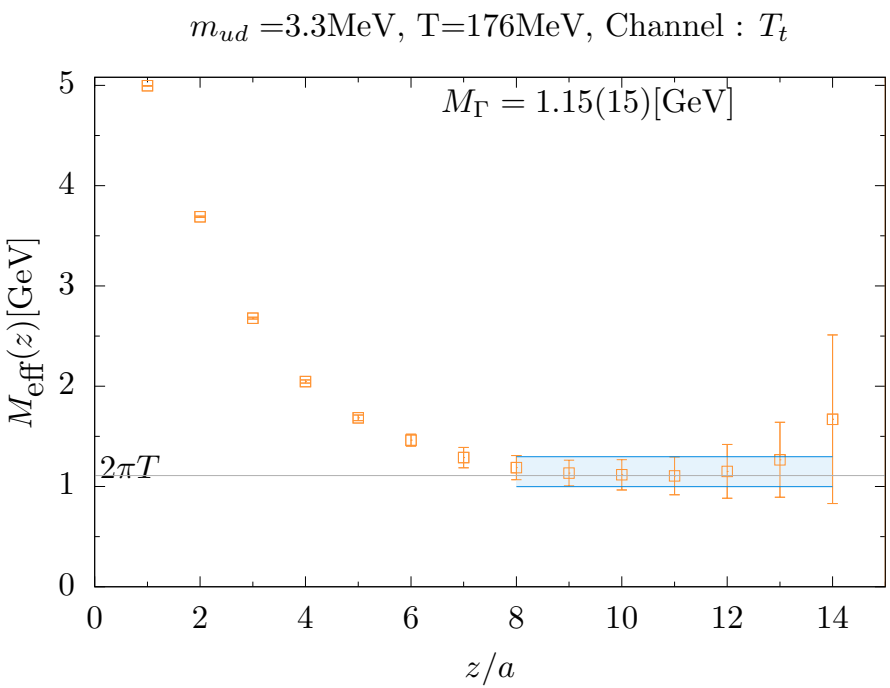

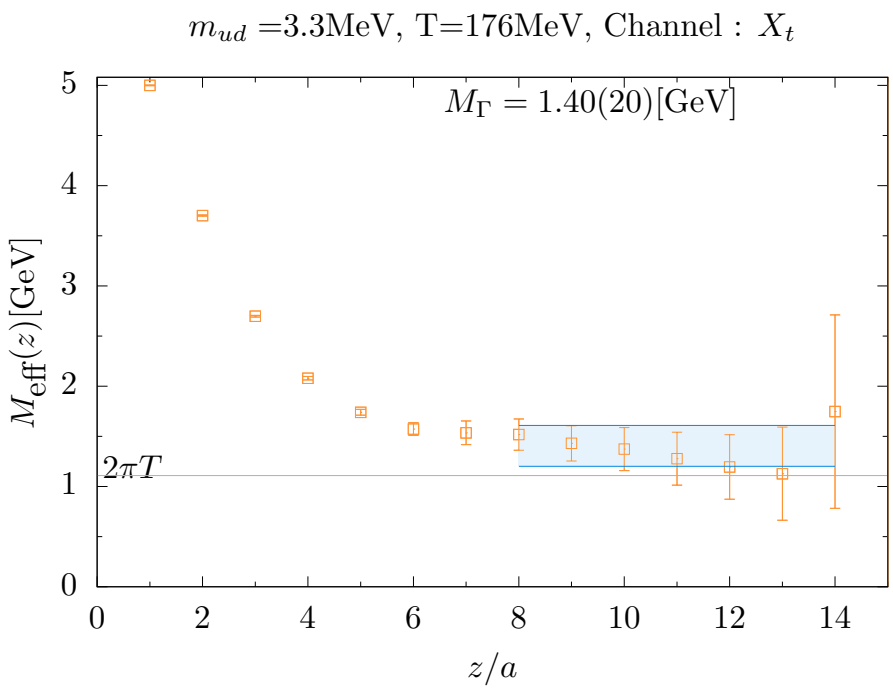

$T = 176$MeV at $m_{ud} = 2.92$MeV

Effective Mass and Fit Range – $SU(2)_L \times SU(2)_R$ – LCP

A_x V_x

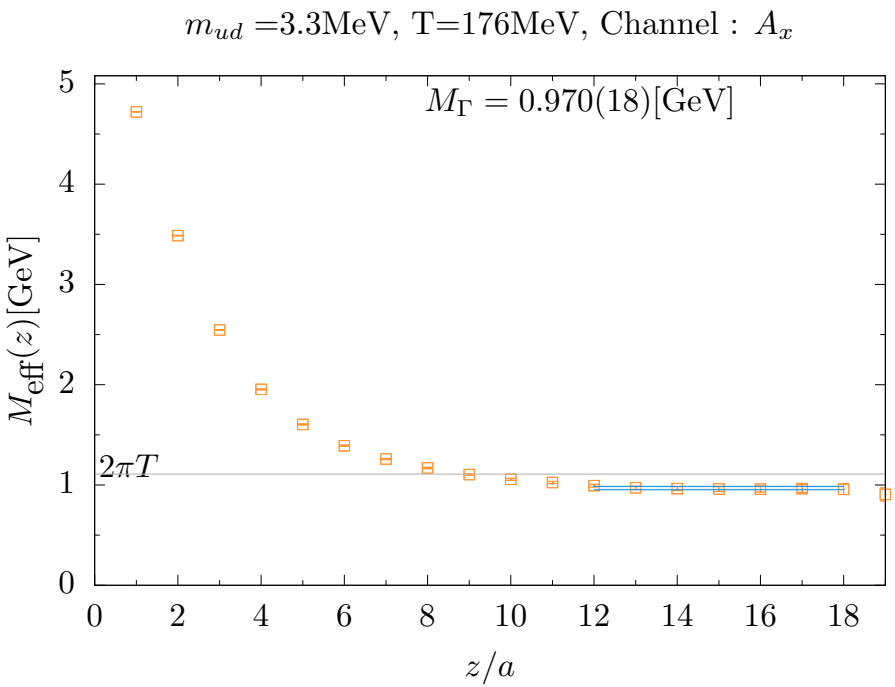

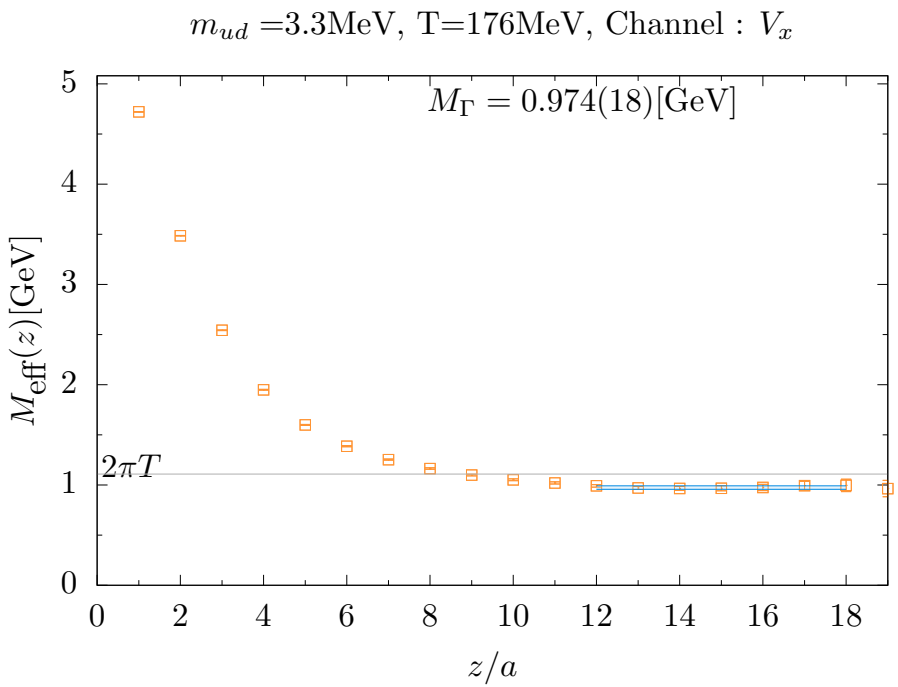

$T = 176$MeV at $m_{ud} = 2.92$MeV

Line of Constant Physics : $36^3 \times 12$

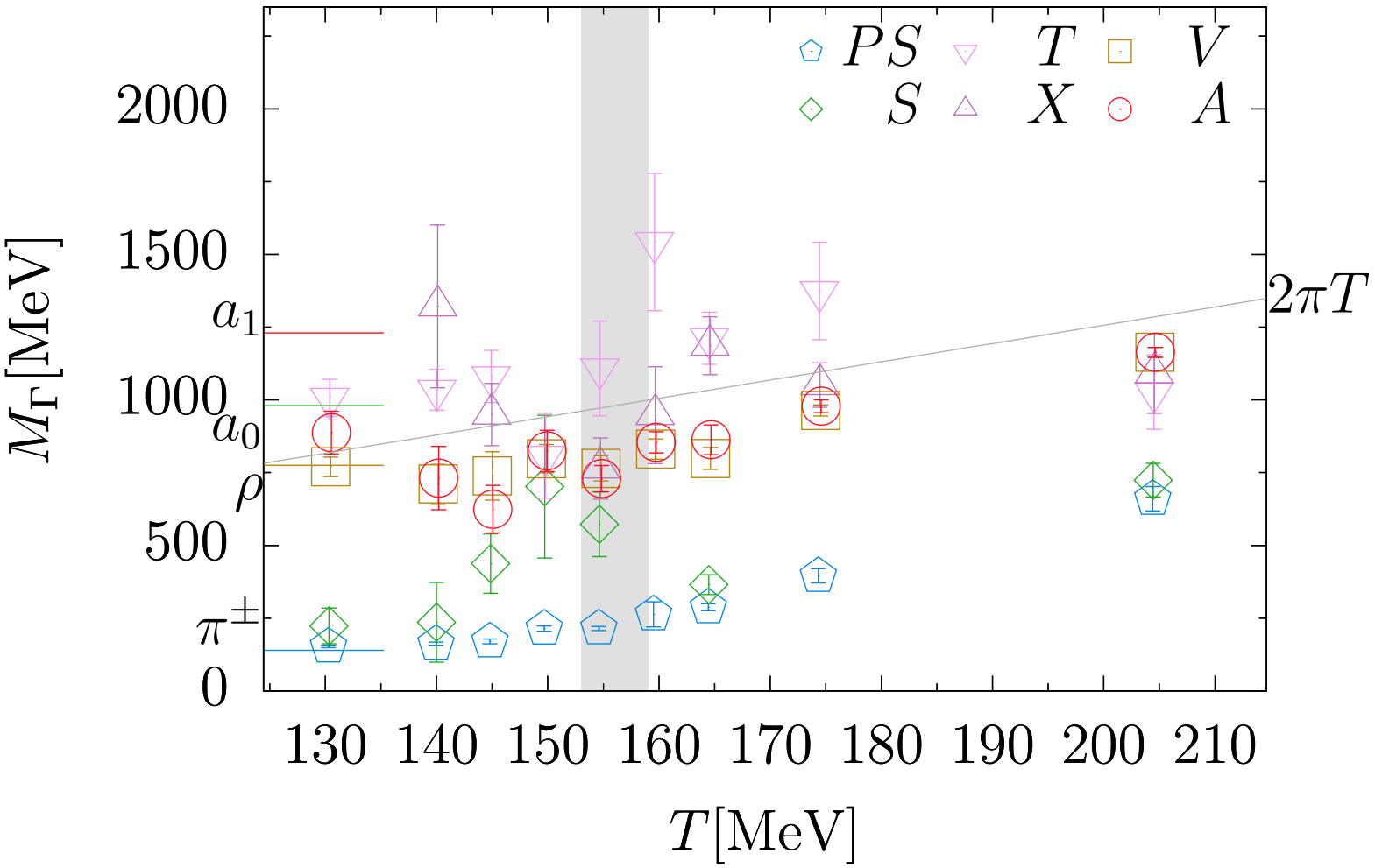

Previous chiral symmetry studies by JLQCD

Previous to this work JLQCD has studied chiral symmetry using several observables:

- Susceptibilities - Topological susceptibility, connected and disconnected susceptibilities.
- Differences in the meson susceptbilities for isospin triplet and singlet states.
- Spectral function analysis from the Overlap and Effective 4D Möbius Domain Wall operators.
- Short range correlations through "current" correlators.
- Two point bilinear correlation function.
- Proportion of two point correlation function.